

# Thermo-optical effects

Oliver Puncken

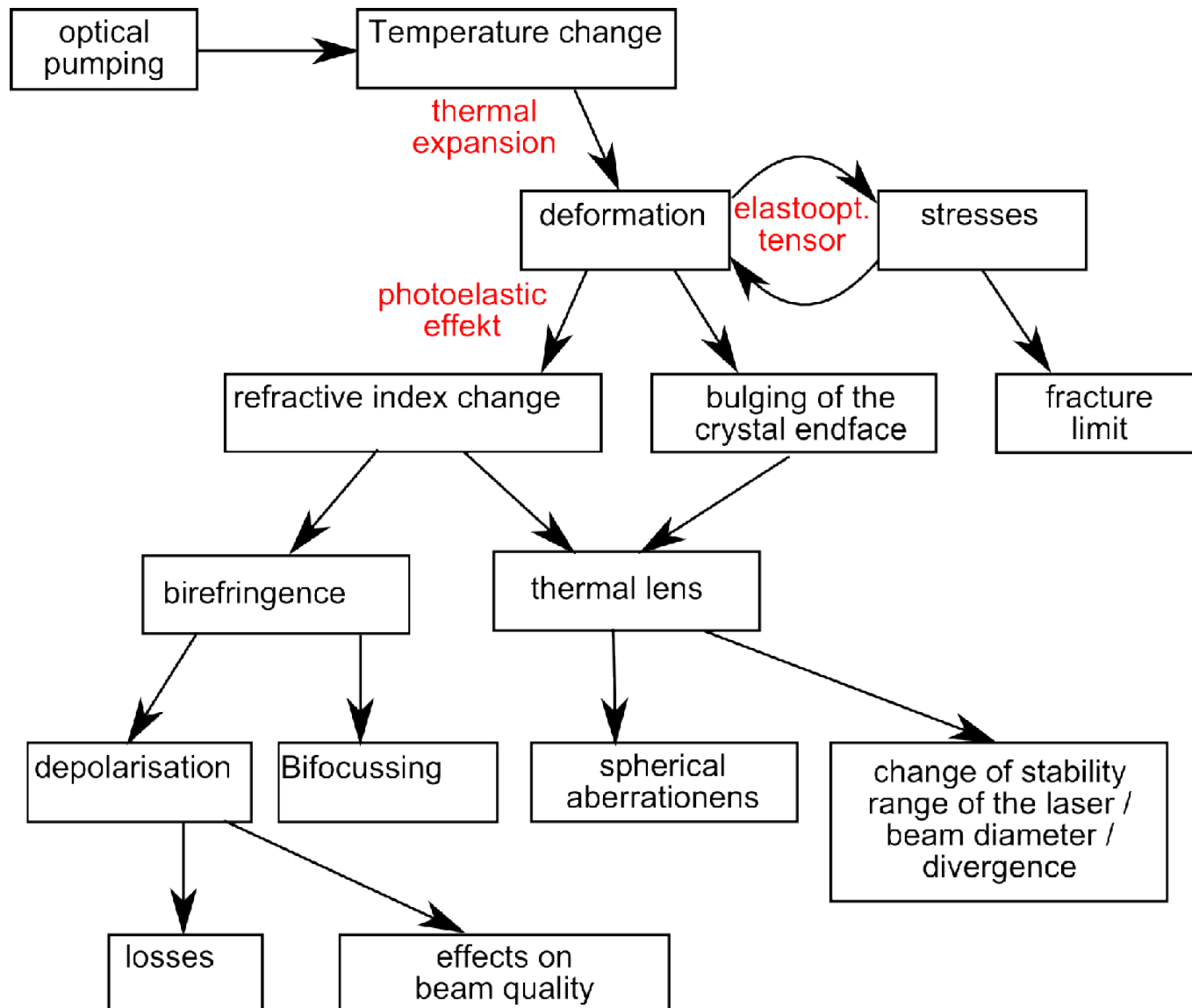
# Outline

- Overview on thermo-optical effects in lasers
  - Thermal lensing
  - Birefringence
  - Depolarization
- Aberrations and the PSL working point
- Attempts for optimization of the PSL laser crystals
  - Different doping concentrations
  - Segmented crystals
  - Intrinsic depolarization compensation

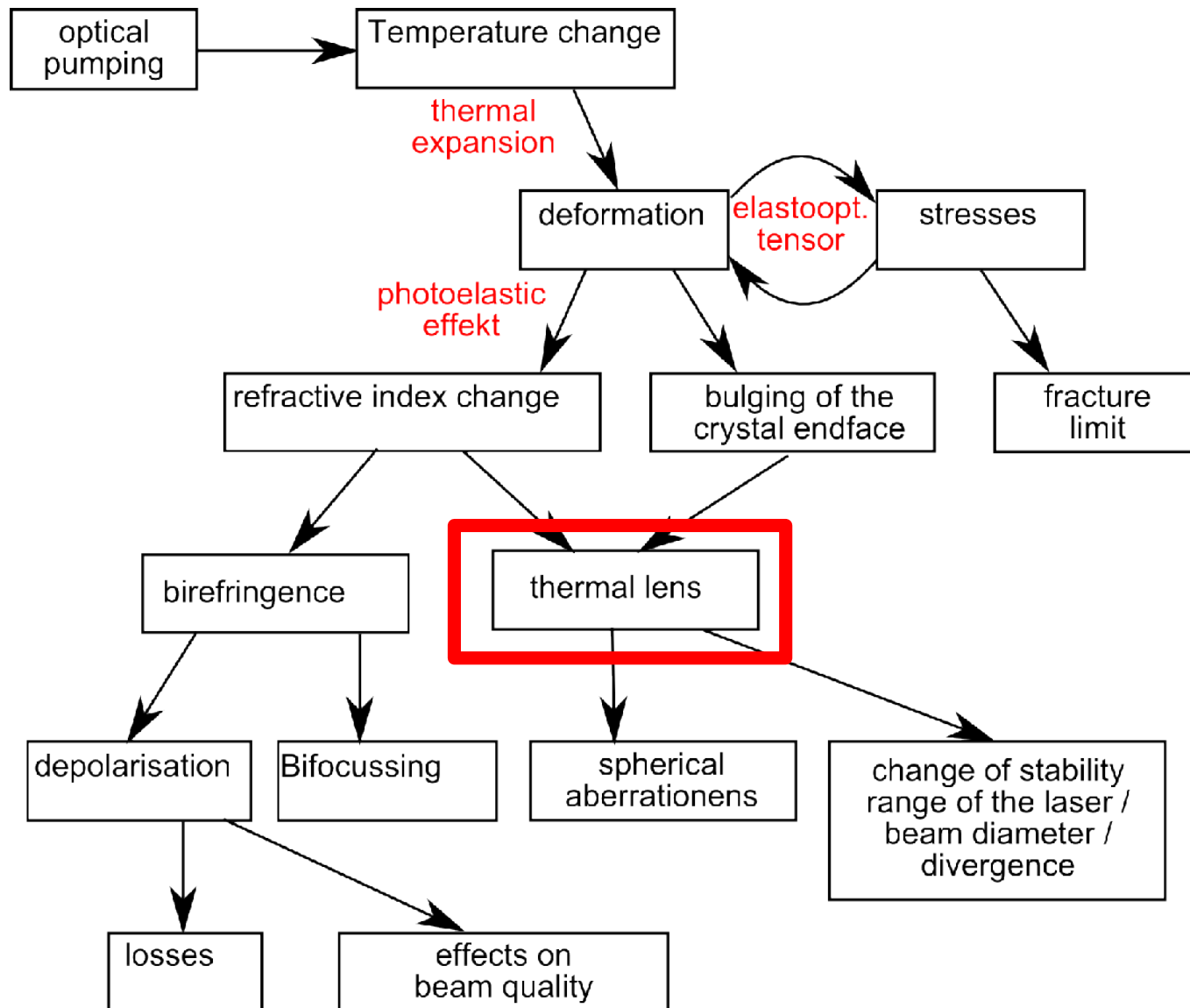
# Outline

- **Overview on thermo-optical effects in lasers**
  - Thermal lensing
  - Birefringence
  - Depolarization
- Aberrations and the PSL working point
- Attempts for optimization of the PSL laser crystals
  - Different doping concentrations
  - Segmented crystals
  - Intrinsic depolarization compensation

# Thermo-optical effects



# Thermo-optical effects



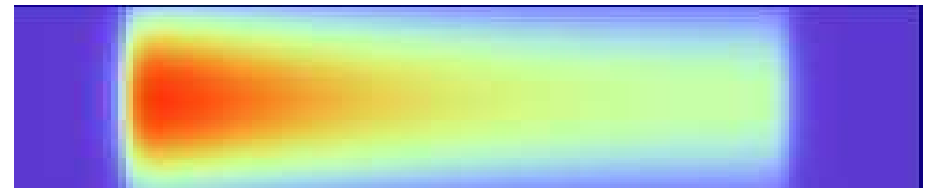
# Thermal lensing

- Pump light is partly converted to heat
- Cooling of barrel → temperature gradient
- Thermal lensing in longitudinal pumped laser rods:

- Time independent heat conduction equation:

$$\nabla^2 T(x,y,z) = -Q(x,y,z) / k,$$

where  $Q$ : thermal energy,  
 $k$ : conductivity



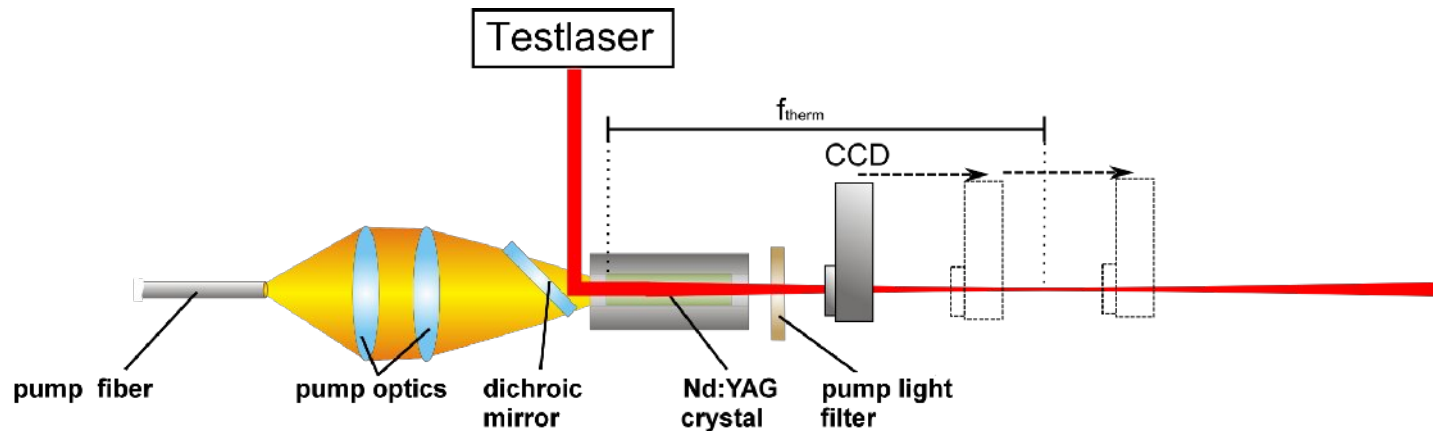
- Refractive index change

$$n(r) = n_0 \cdot (1 - \gamma r^2),$$

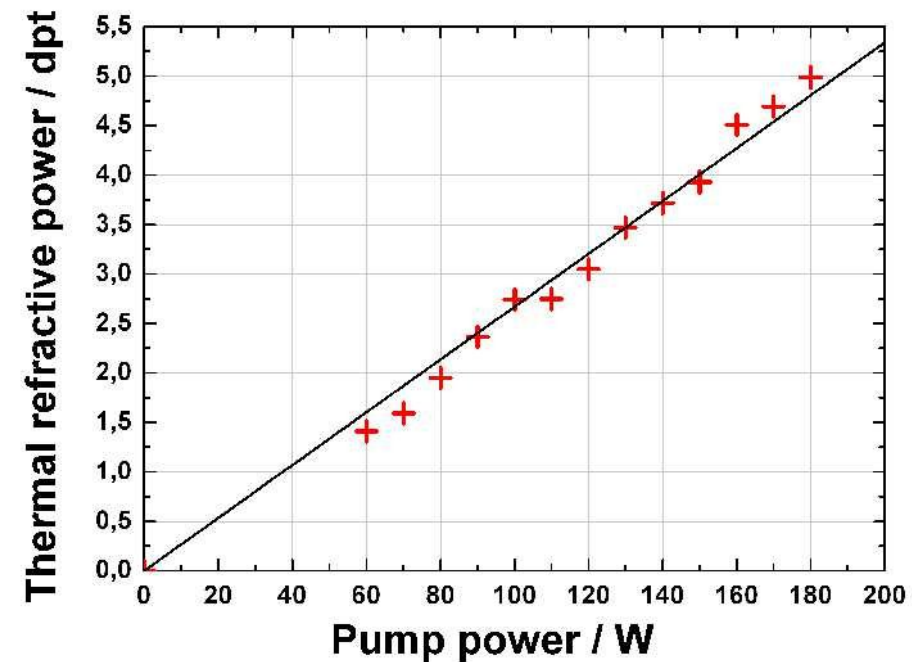
where  $\gamma = \gamma(\text{pump power, created heat, heat conductivity, crystal length, } dn/dT, \dots)$

- → thermal lens with refractive power, which rises linear with the pump power

# Thermal lensing

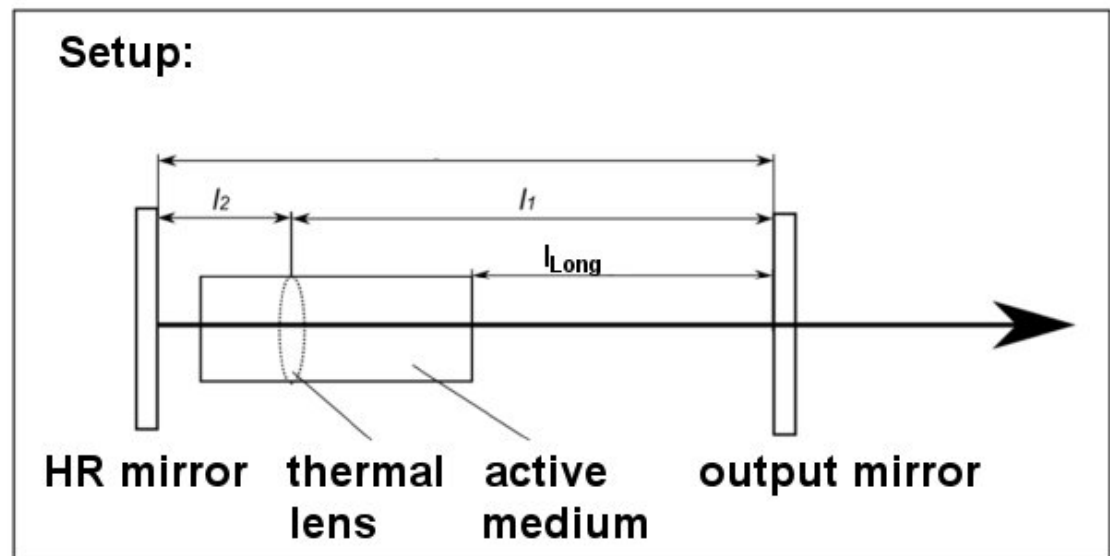
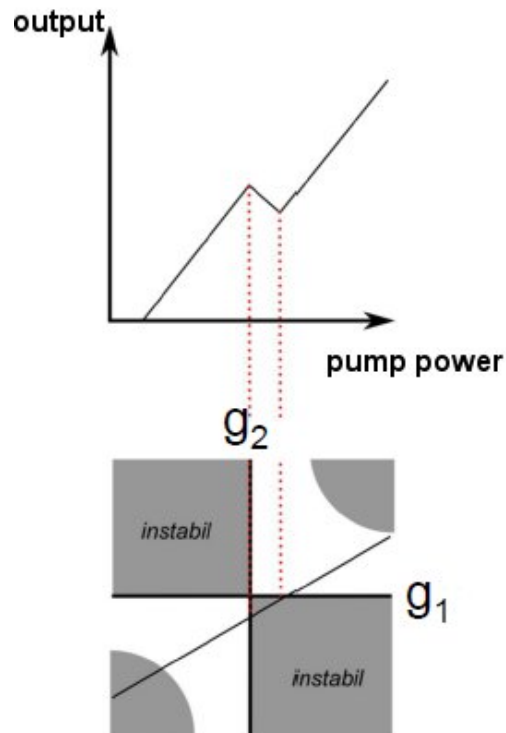


- Testbeam:
  - 980 nm DFB diode, fundamental mode
  - 650  $\mu\text{m}$  beam radius
  - → thermal refractive power of 0.027 dpt/W.



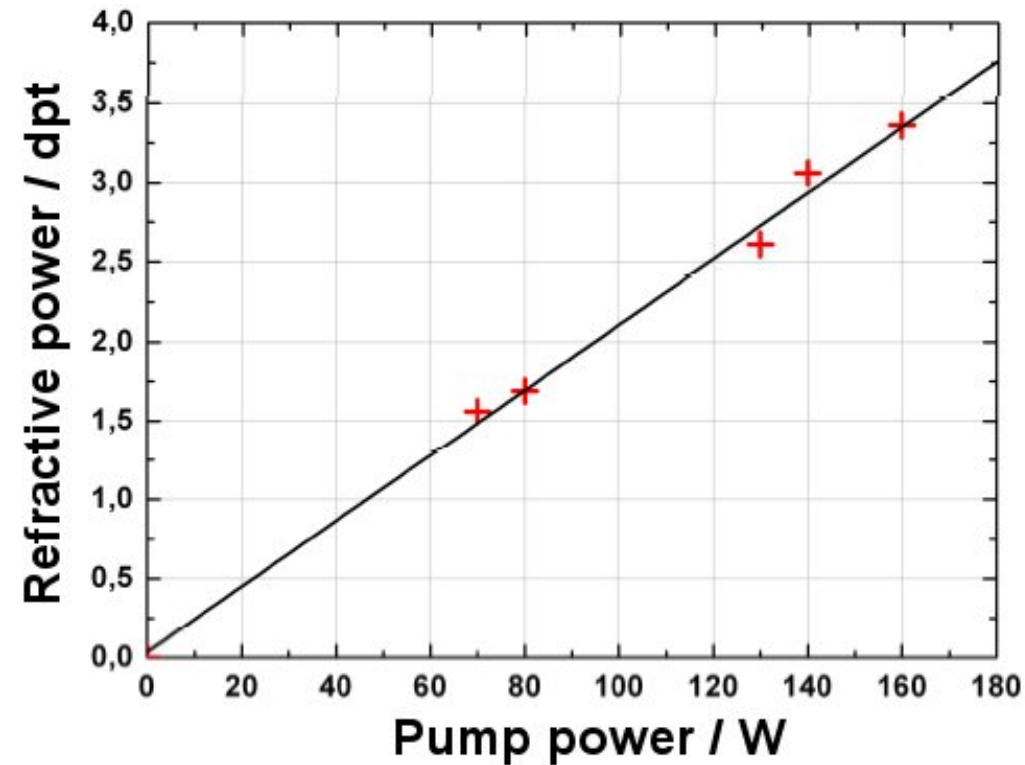
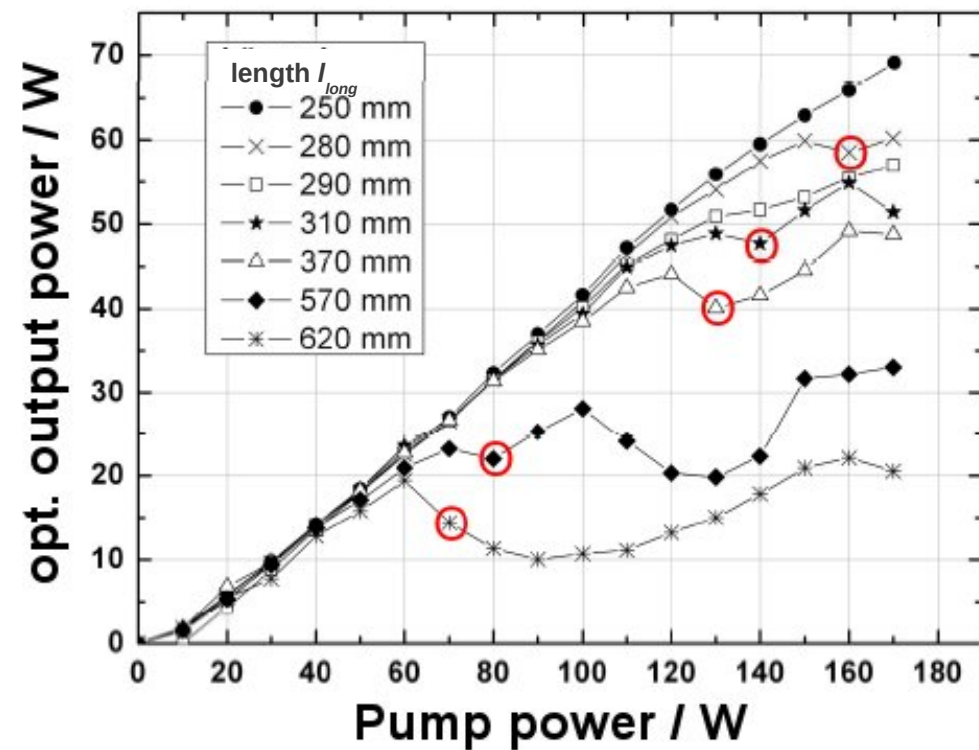
# Thermal lensing

- Laser stability:
  - Increase pump power in asymmetric resonator until it becomes unstable
  - Thermal lens at this point:  $D = 1 / ( l_{long} + L / (2n) )$





# Thermal lensing

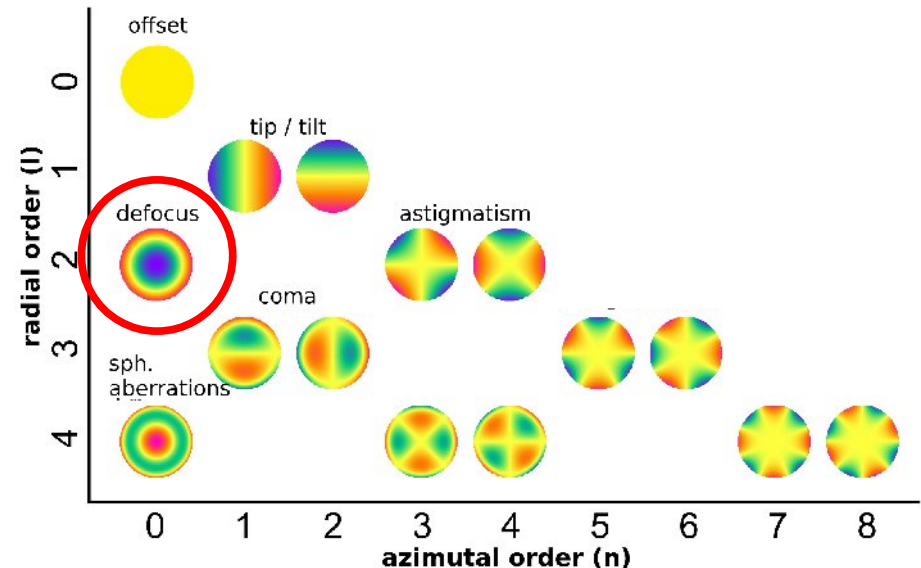
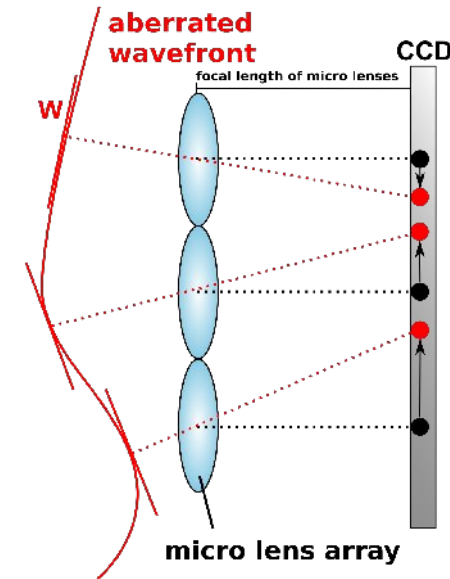


- Thermal refractive power: 0.021 dpt/W

# Thermal lensing

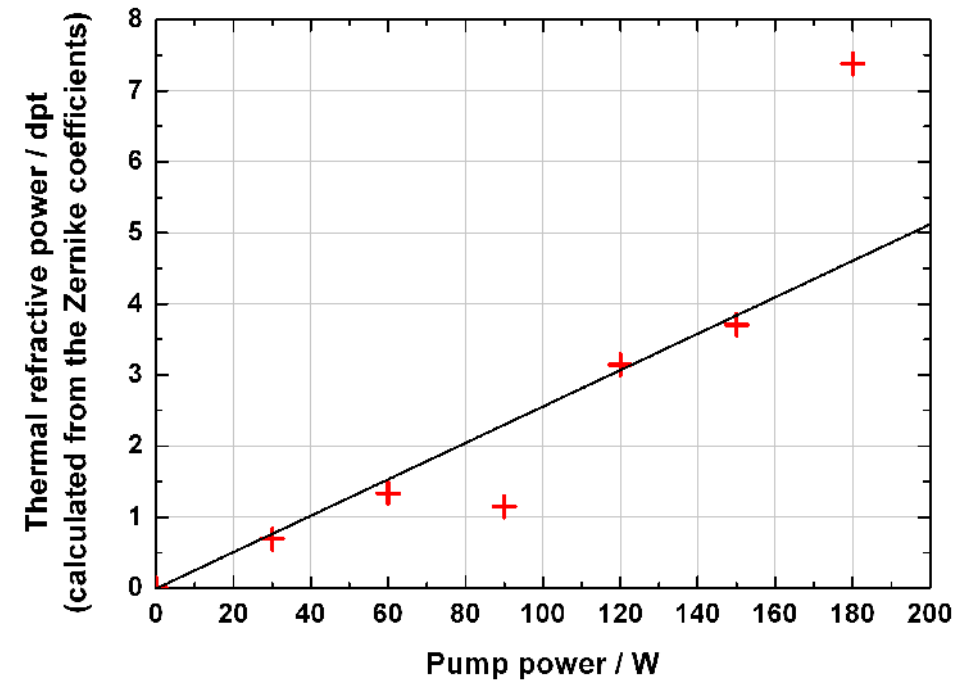
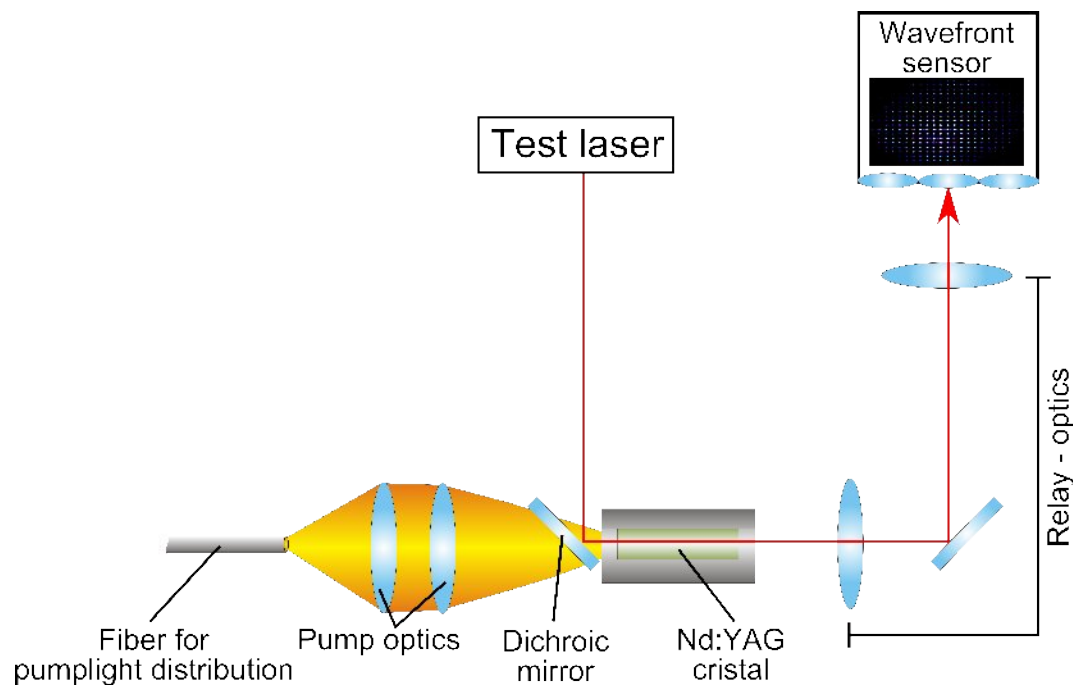
- Wavefront sensor
  - Quite sensitive for fluctuations → big errors
  - Thermal refractive power from Zernike defocus coefficient  $c_{20}$ :

$$D = 4 \cdot c_{20} \cdot \lambda / r_0^2$$



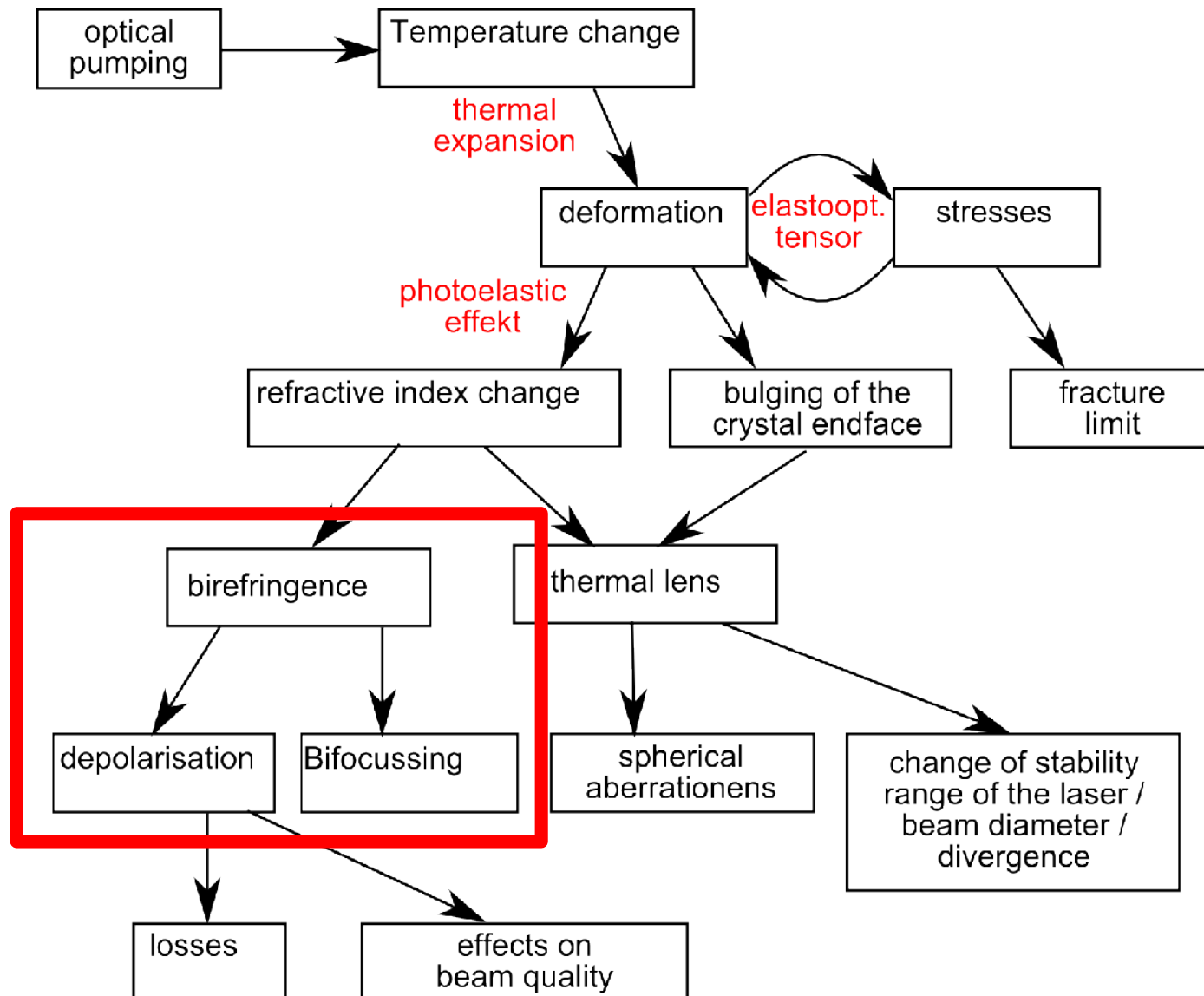
# Thermal lensing

- Wavefront sensor



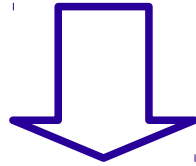
Refractive power:  
about 0.025 dpt/W

# Thermo-optical effects

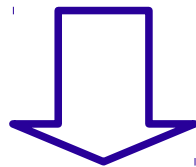


# Birefringence and bifocussing

Heating power

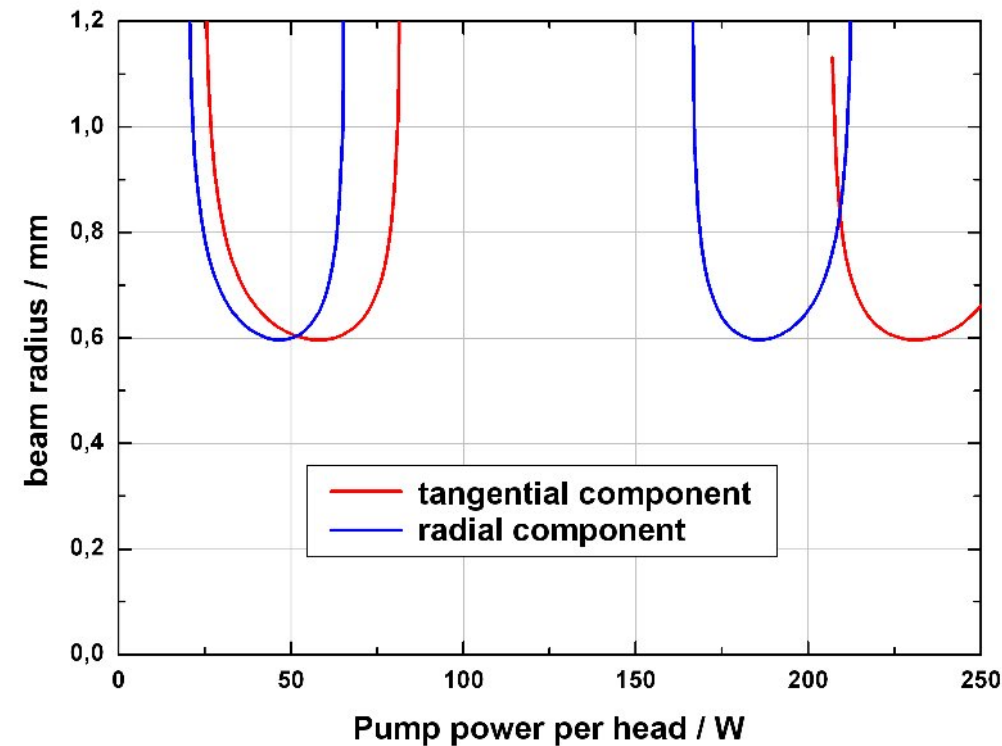


Different refractive indices for radial and tangential polarization components of the laserlight (birefringence)



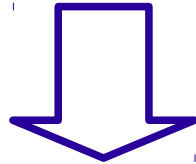
**Bifocussing**

Effect on the mode radius of an asymmetric two head resonator

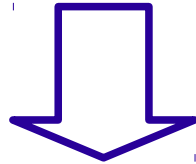


# Birefringence and bifocussing

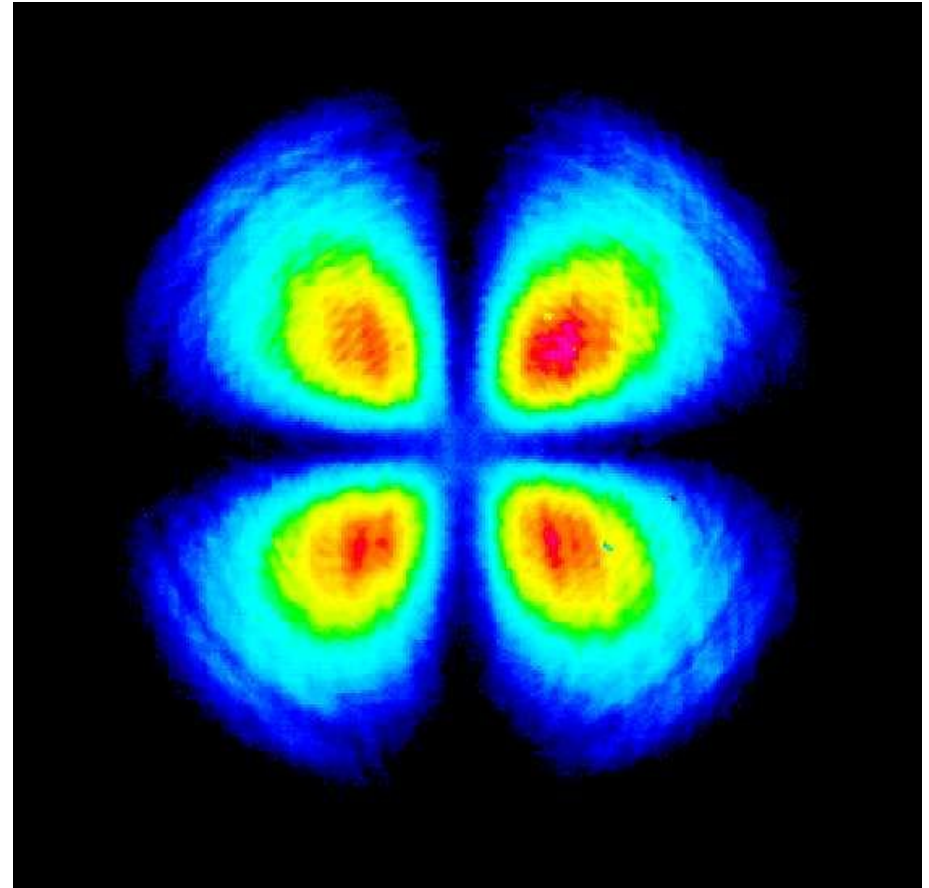
Heating power



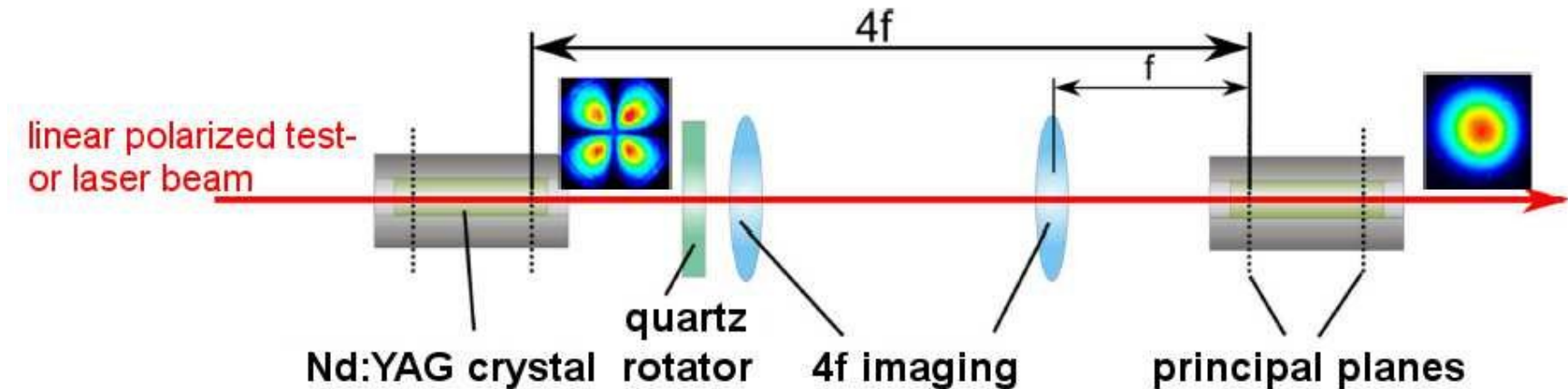
Different refractive indices for radial and tangential polarization components of the laserlight  
(birefringence)



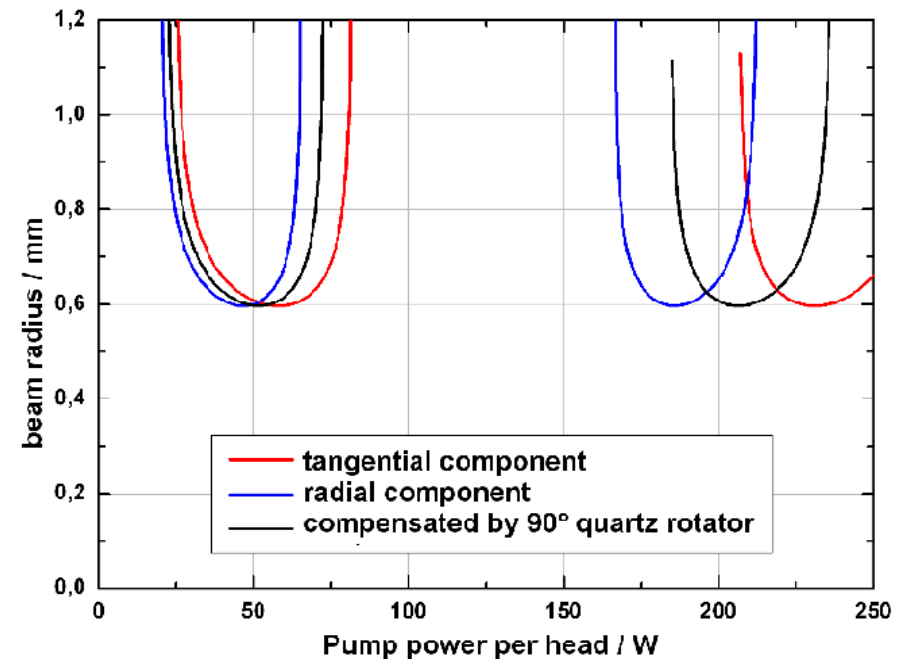
**Phase shift** for pol. components depends on the radial position → **Depolarization**



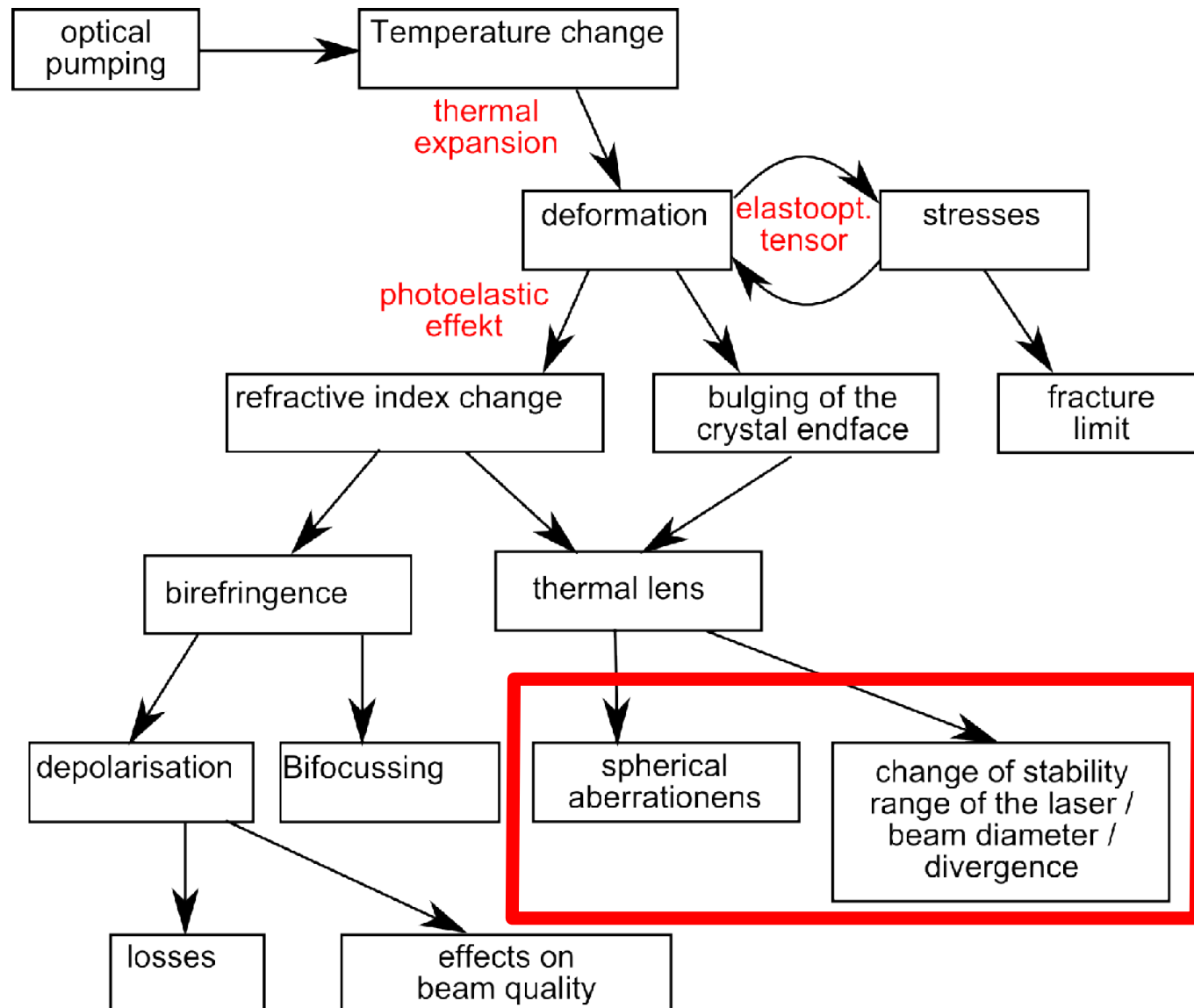
# Birefringence compensation



- Principle:
  - Exchange polarization components by  $90^\circ$  rotation between crystal passes
  - Imaging of the thermal lens' principal planes results in compensation of phase shifts



# Thermo-optical effects





# Outline

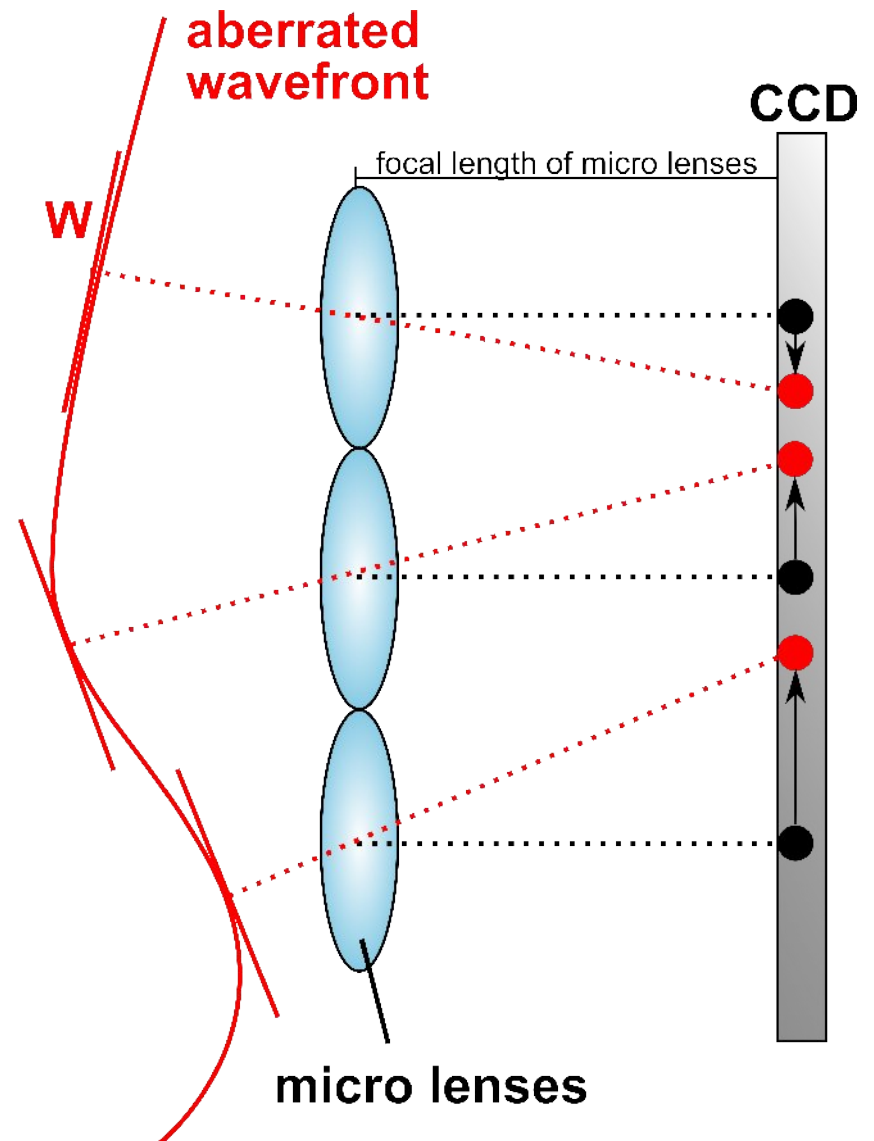
- Overview on thermo-optical effects in lasers
  - Thermal lensing
  - Birefringence
  - Depolarization
- **Aberrations and the PSL working point**
- Attempts for optimization of the laser crystals
  - Different doping concentrations
  - Segmented crystals
  - Intrinsic depolarization compensation

# Aberrations

- Thermal lens as a result of absorption of pump- (and laser-) light
- For homogenous pumplight distribution: radially parabolic temperature profile
- For radially inhomogenous pumplight distribution: radially parabolic temperature profile might be roughly true, but (mainly spherical) aberrations appear

# Measurement of aberrations

- Shack Hartmann sensor
  - The lateral position of a (micro-) lens spot depends on the mean slope of the incoming wavefront
  - The mean slope of the wavefront can be calculated from the spot-displacement



# Zernike Polynomials

- The optical path difference of a wavefront  $W$  can be developed as a sum of polynomials and their coefficients
- Zernike polynomials are common, because each polynom correspond to a kind of aberration

$$W(\rho, \theta) = \lambda \cdot [c_{00} + \sum_{n=1}^{\infty} \sum_{l=-n}^n c_n Z_n^l]$$

Azimuthal order  $\rightarrow$

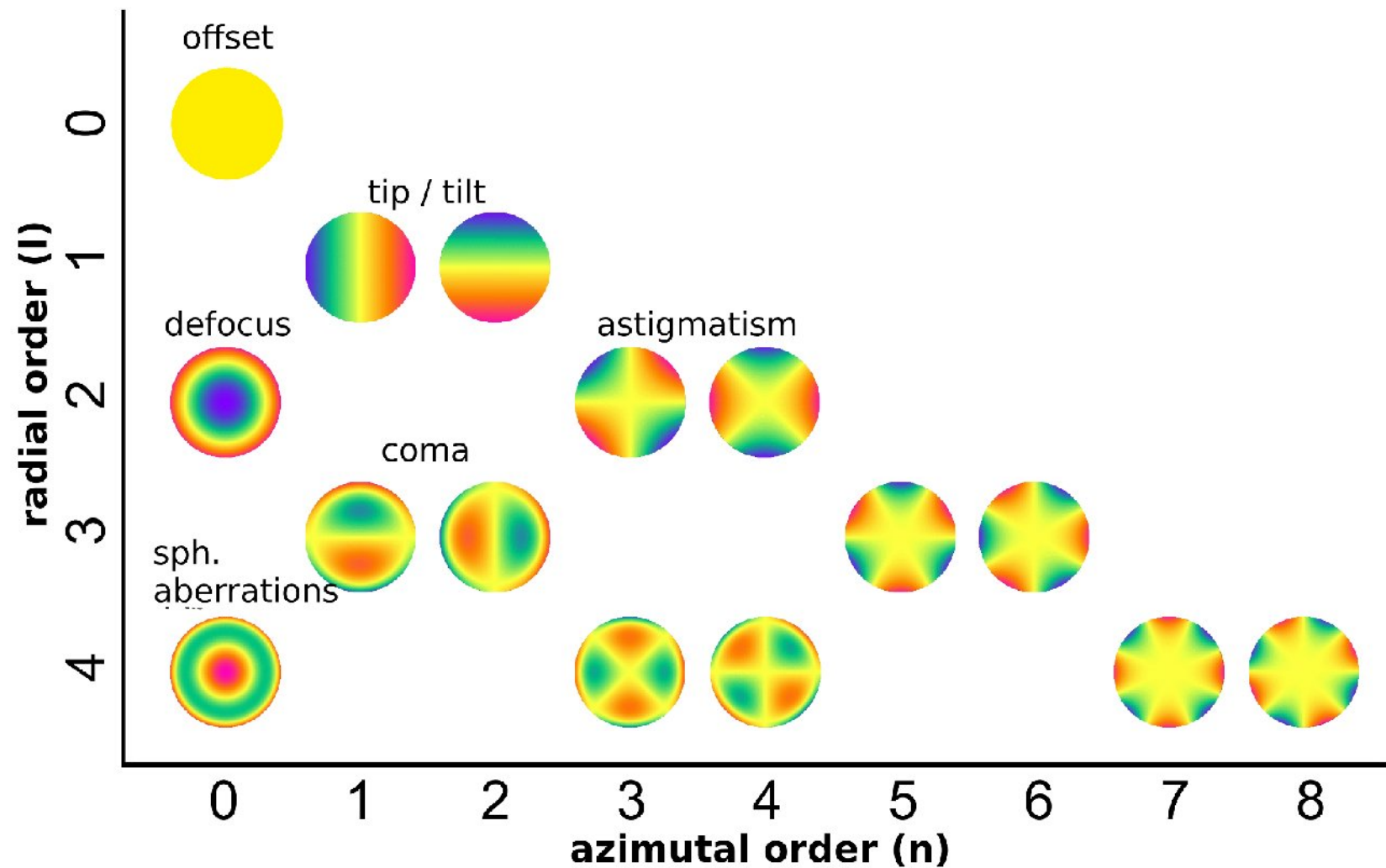
$$Z_n^l = R_n^m(\rho) \cdot \cos(m \cdot \theta), \text{ if } l > 0$$
$$Z_n^l = R_n^m(\rho) \cdot \sin(m \cdot \theta), \text{ if } l < 0$$

Radial order  $\rightarrow$

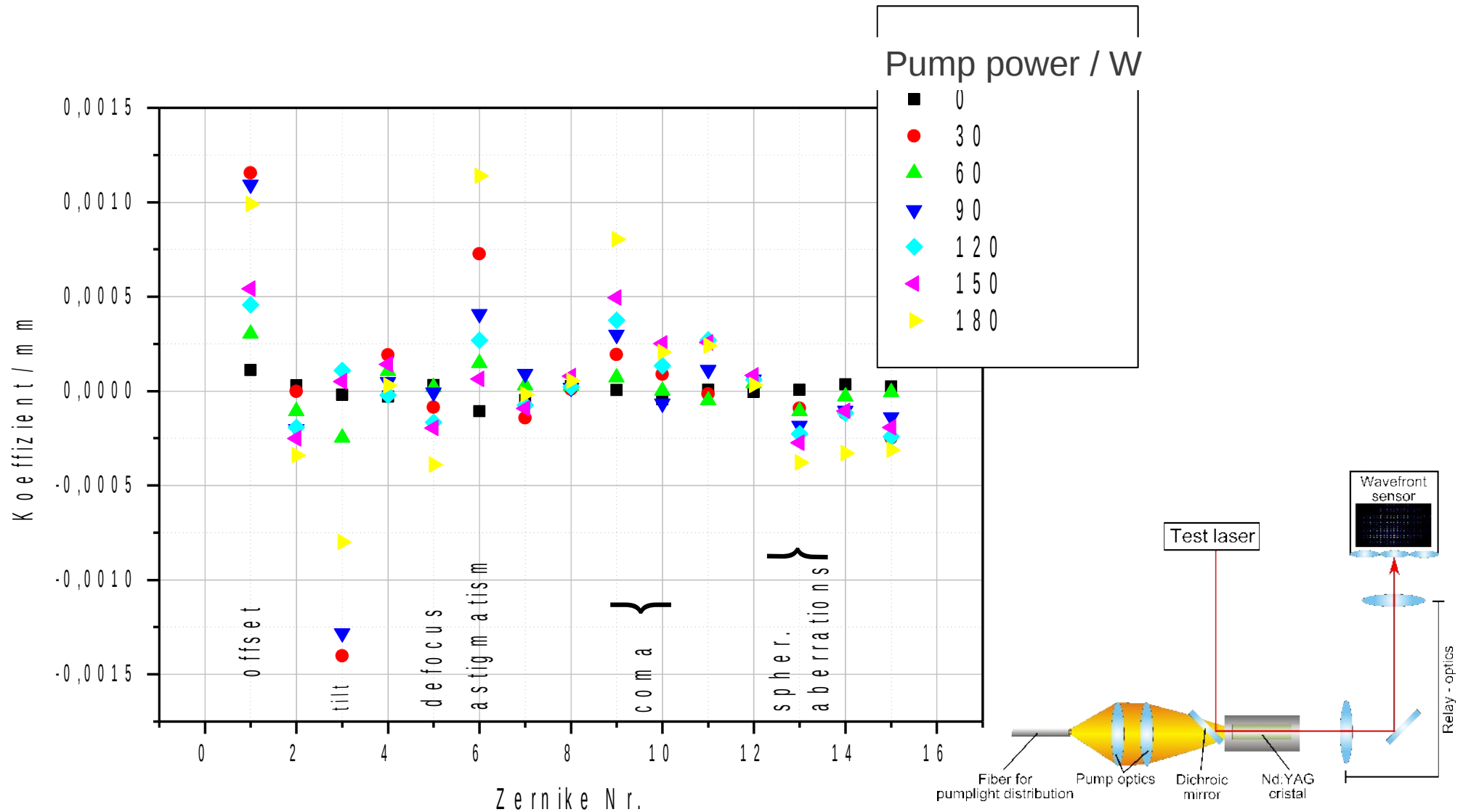
Radial polynomial  $\rightarrow$

angular function  $\rightarrow$

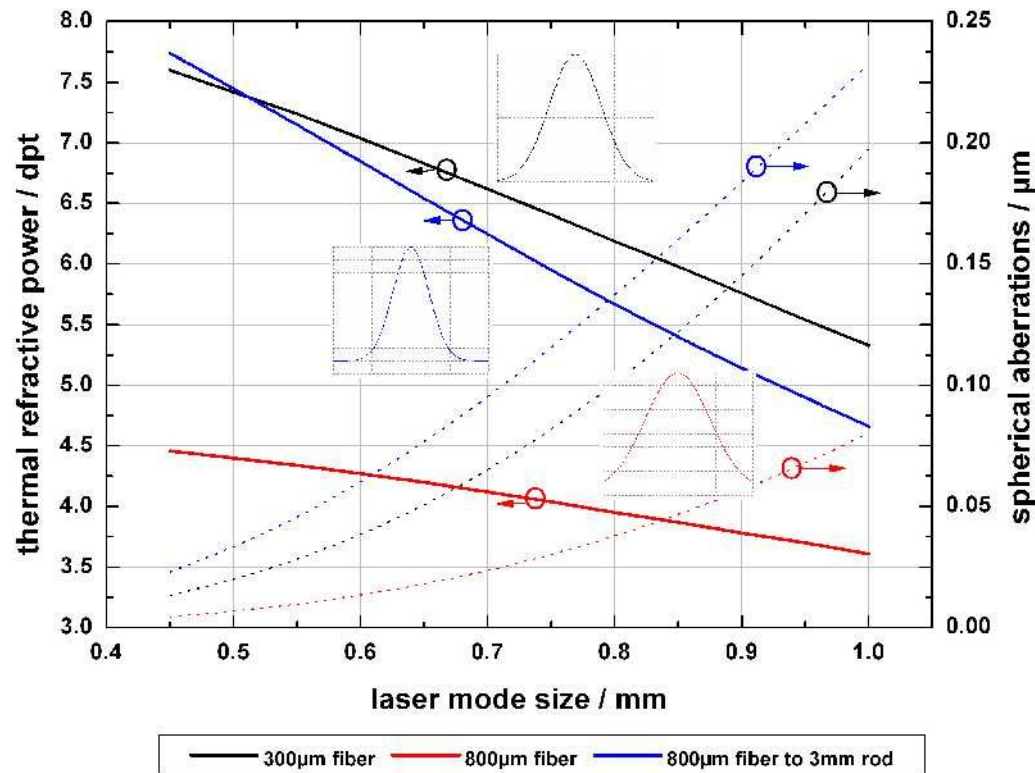
# Zernike Polynomials



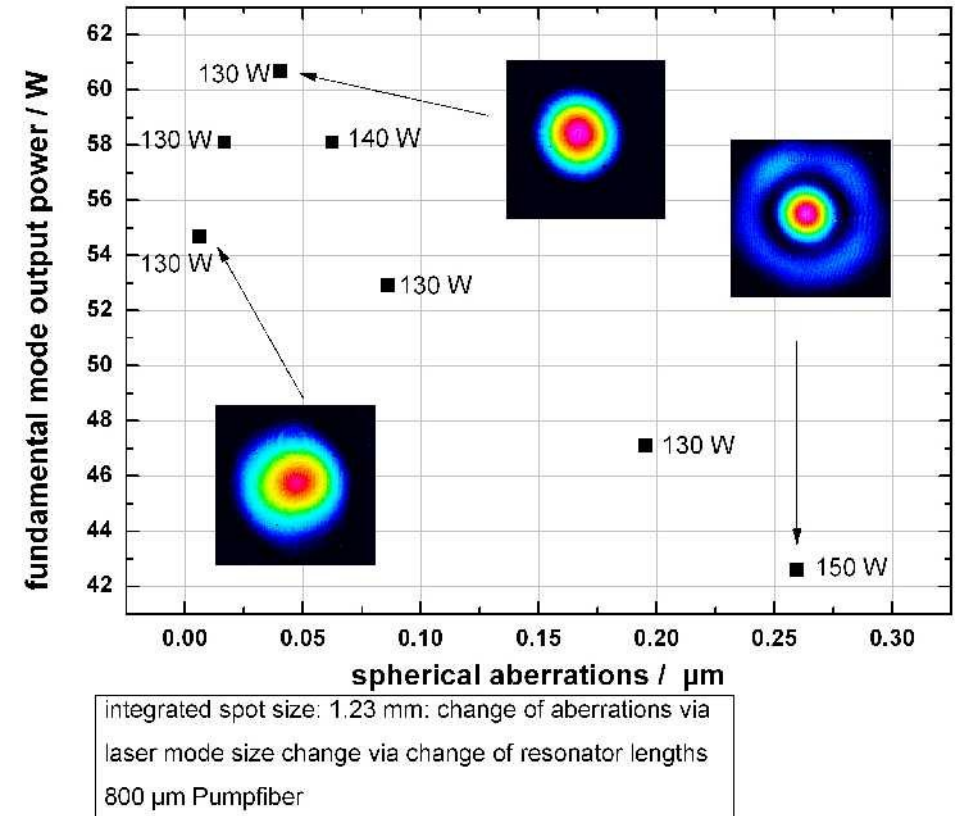
# Test setup – Results for LIGO xtal



# Experimental investigations



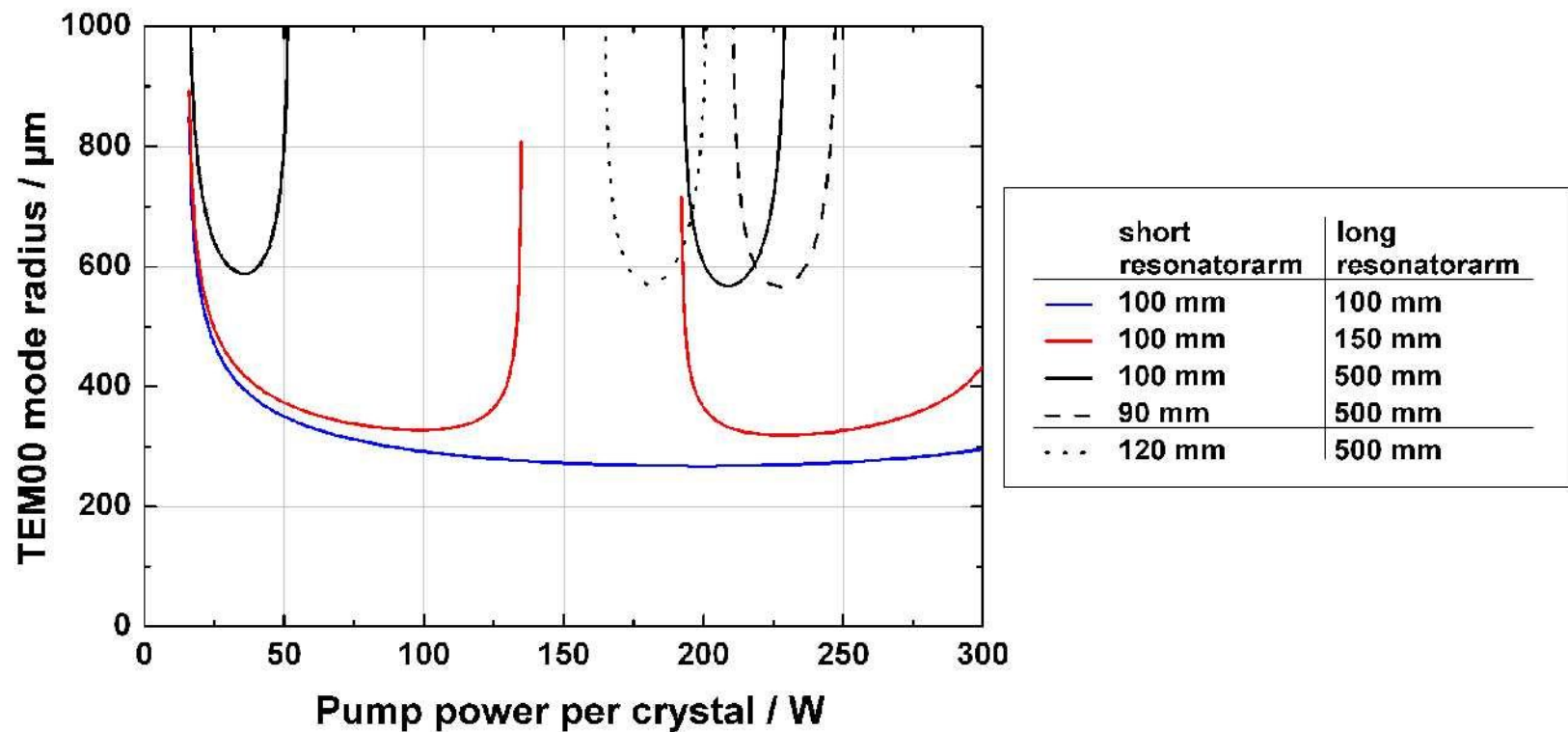
The smaller the laser mode size, the higher the thermal refractive power (defocus), but the lower the spherical aberrations



Influence of spherical aberrations on beam profile

# Effects on the PSL working point

- Asymmetric resonator splits the stability range into two parts with respect to the pump power

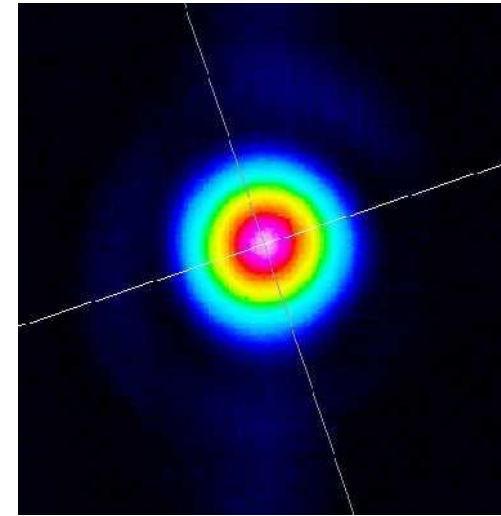
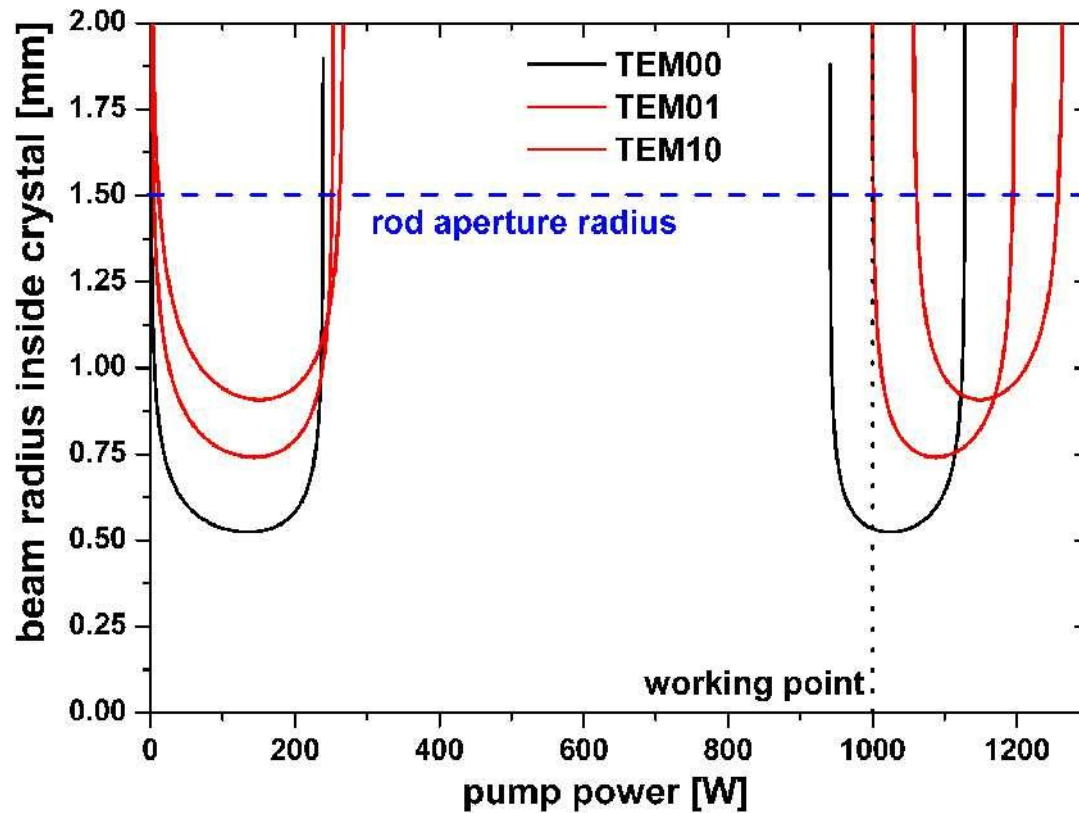




# Effects on the PSL working point

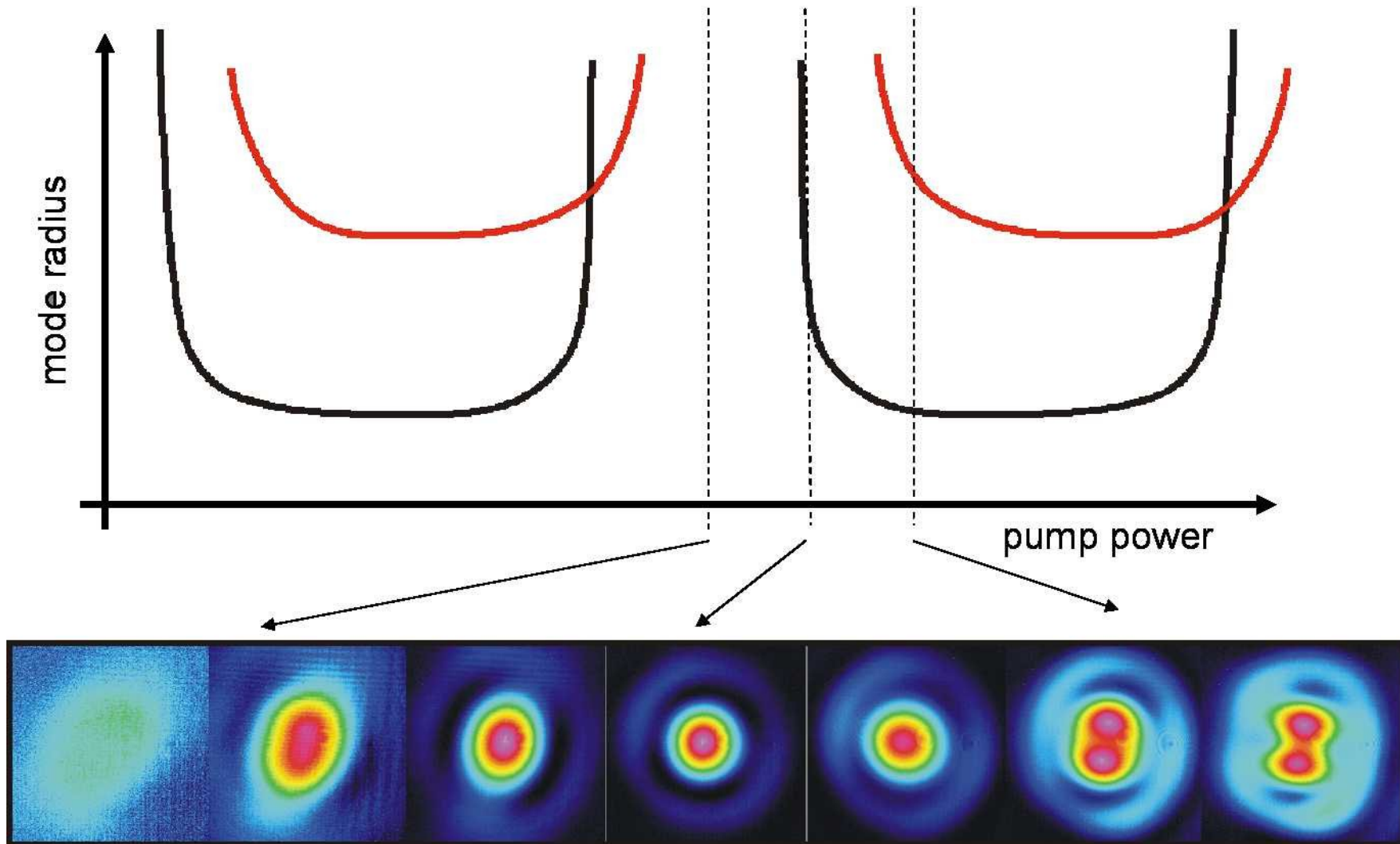
- Asymmetric resonator splits the stability range into two parts with respect to the pump power
- Spherical aberration are used as control mechanism for TEM<sub>00</sub> working point:  
Higher order modes experience a lower effective thermal lens!

# Effects on the PSL working point



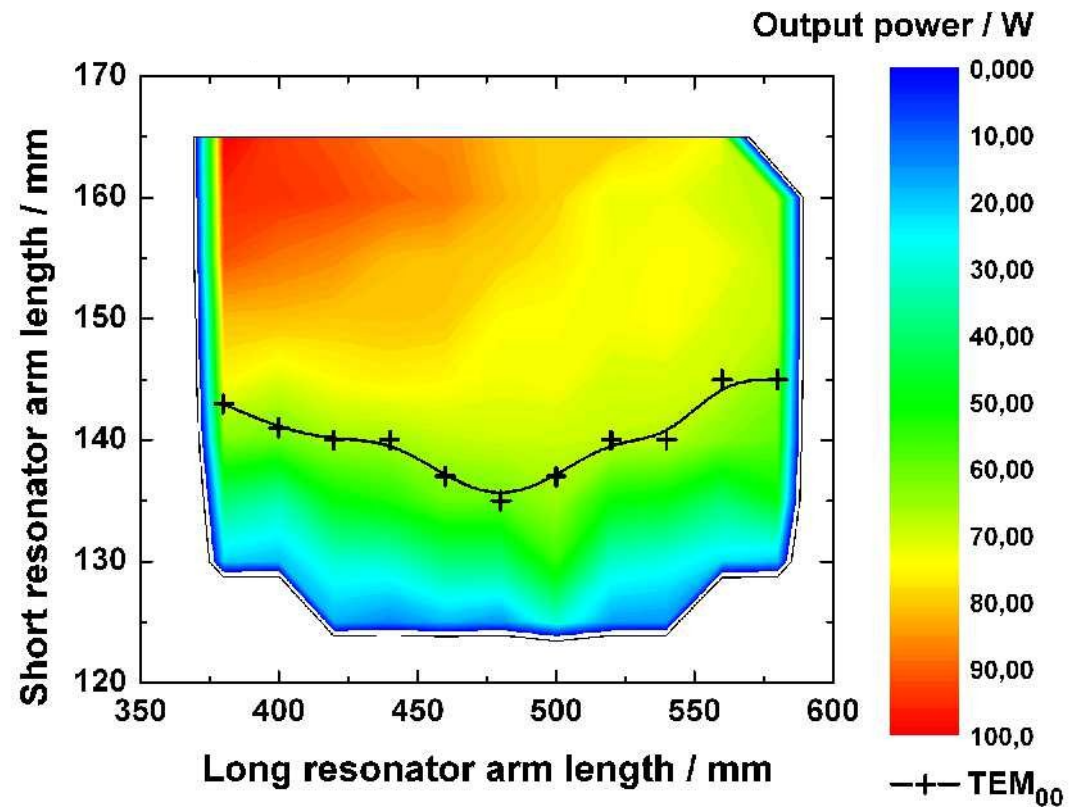
- Laser mode radius in first crystal
- Mode radius = stability criterium
- Higher order modes → larger radius
- Aberrations of the thermal lens → HOM shifted towards higher pump powers
- Values derived by an ABCD calculation of the actual resonator including the thermal lens
- Output beam profile of the free running laser oscillator at an output power of 176 W

# Effects on the PSL working point



# Experimental experiences (2-head resonator)

- Birefringence compensated two head resonator
- 0.1 at.% doped crystals
- 200W pump power per crystal
- Homogenizer, 2mm diameter

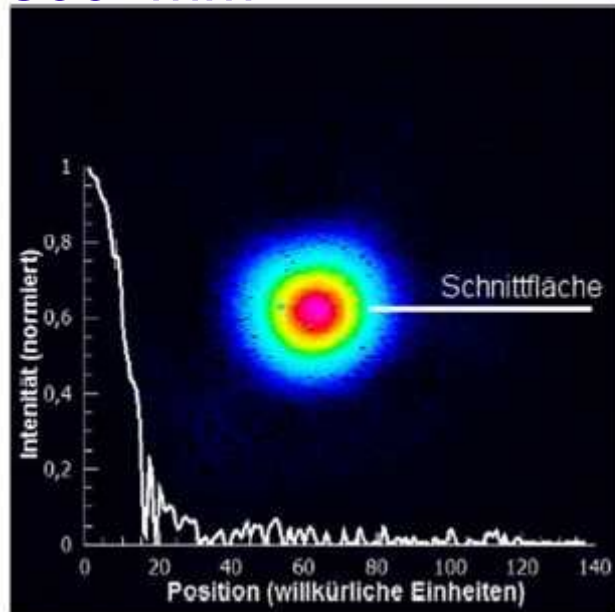


# Experimental experiences (2-head resonator)

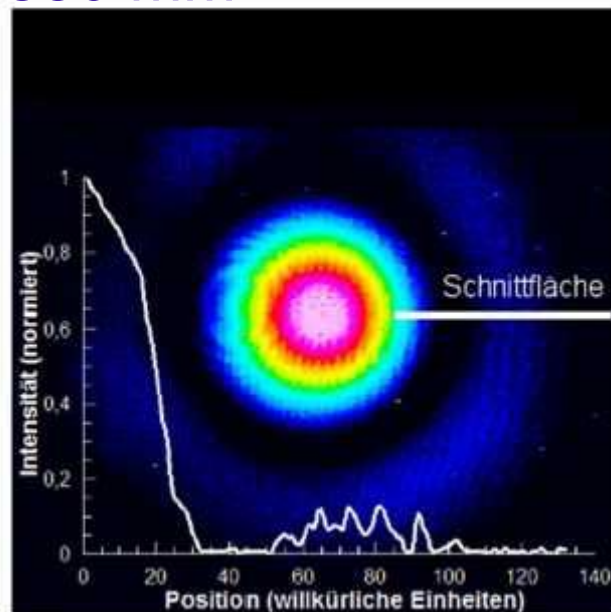
- 200W pump power per crystal
- Length of the short resonator arm: 130 mm

Length of the long resonator arm:

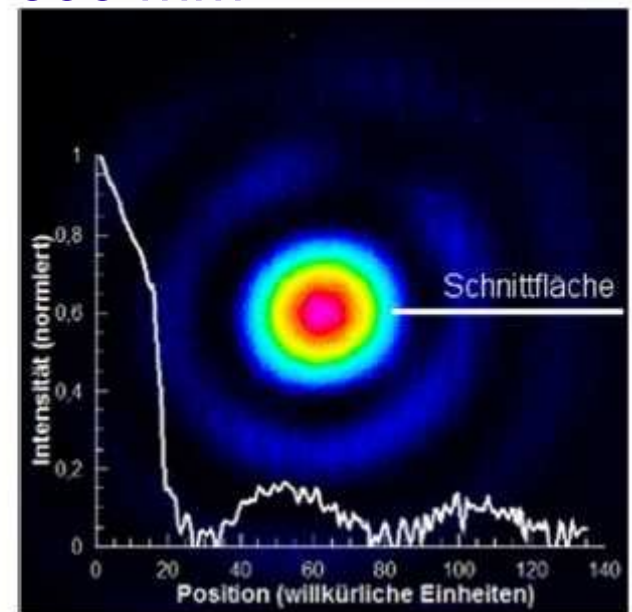
500 mm



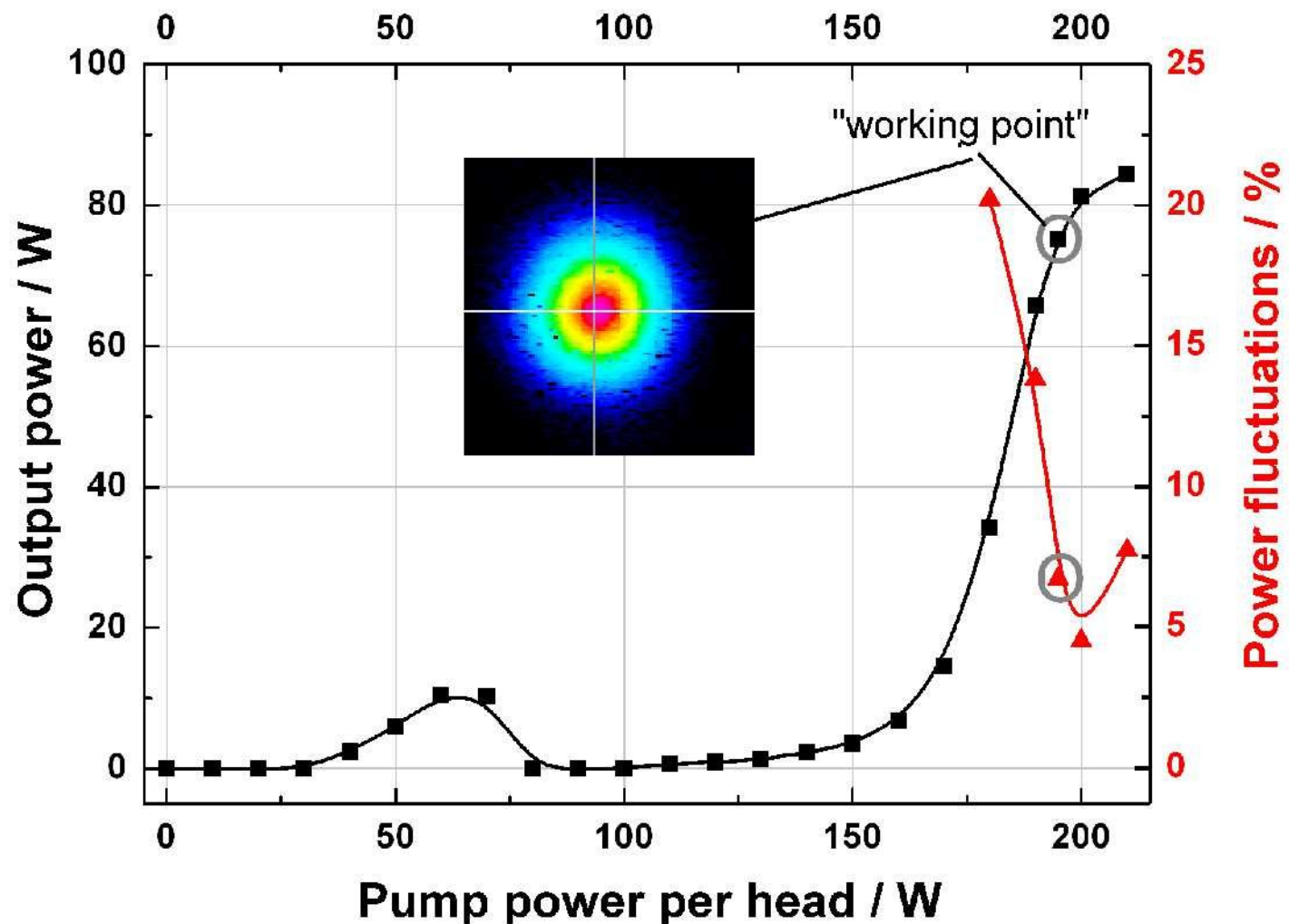
550 mm



600 mm

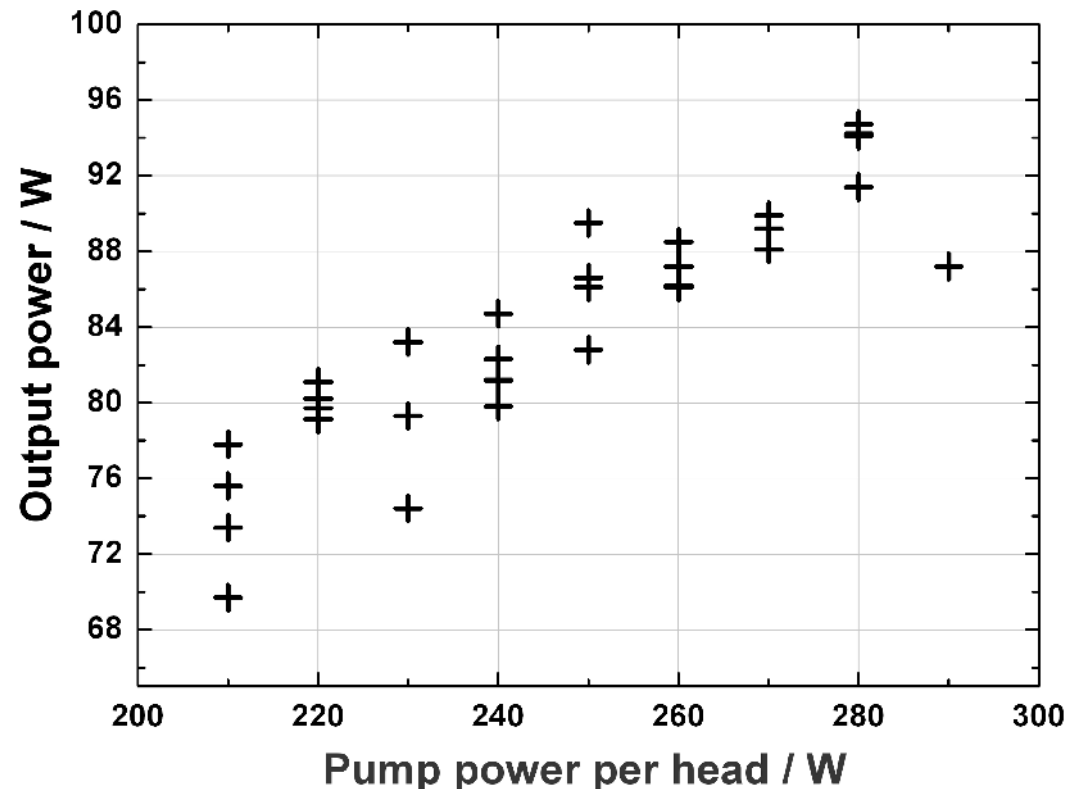


# Experimental experiences (2-head resonator)



# Power scaling (2-head resonator)

- In general:  
More pump power  
→ more output power
- Adapt resonator to get TEM<sub>00</sub>-operation
- Limits:
  - pump power
  - mechanics





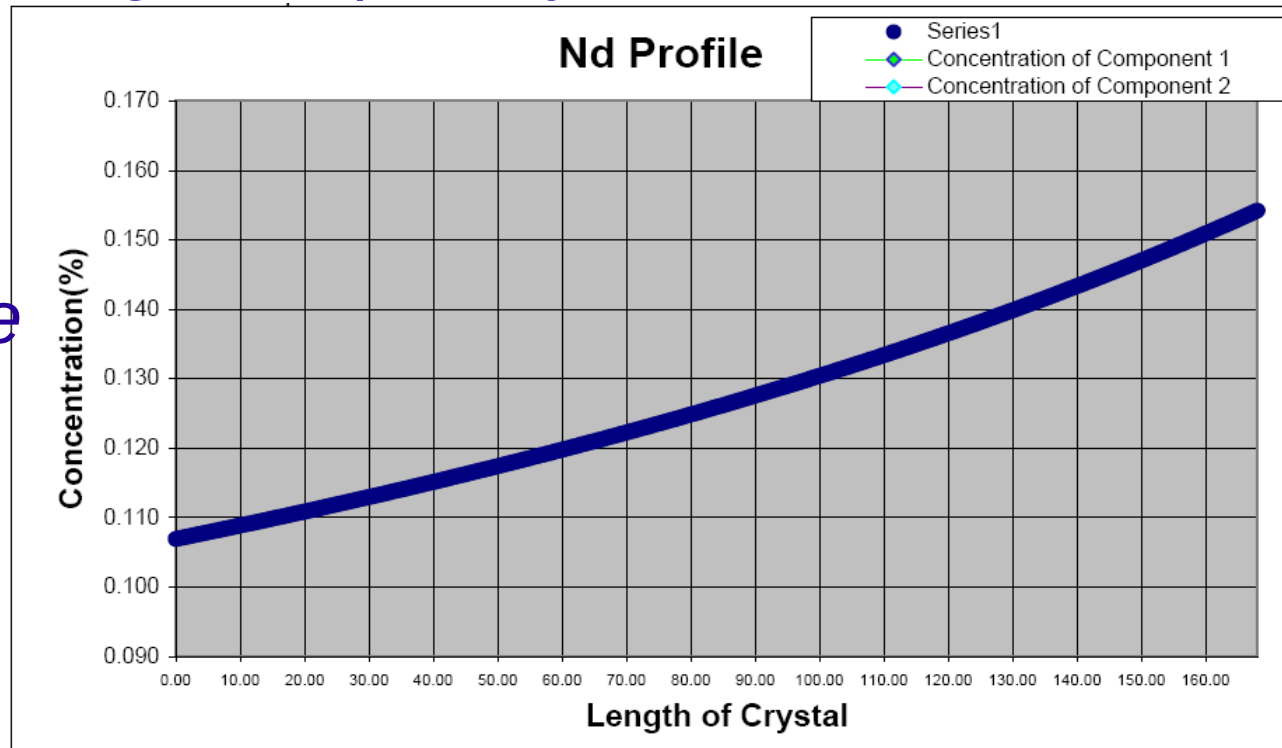
# Outline

- Overview on thermo-optical effects in lasers
  - Thermal lensing
  - Birefringence
  - Depolarization
- Aberrations and the PSL working point
- **Attempts for optimization of the laser crystals**
  - **Different doping concentrations**
  - Segmented crystals
  - Intrinsic depolarization compensation



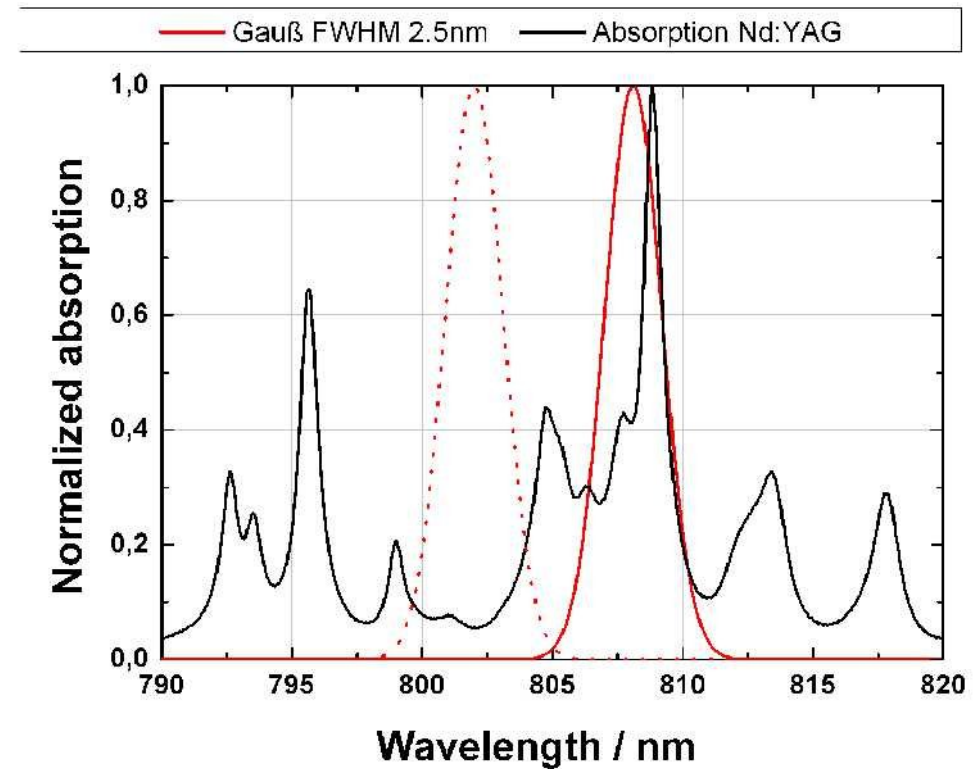
# Highly doped crystals

- Typical accuracy in Nd:YAG doping specified as 0.01 at.%
  - 10% for 0.1 at.% doped crystals
  - 1% for 1 at.% doped crystals
    - The properties of higher doped crystals are more reliable
- Manufacturing process causes a longitudinal *absolute* doping gradient
- Higher doped crystals are more common



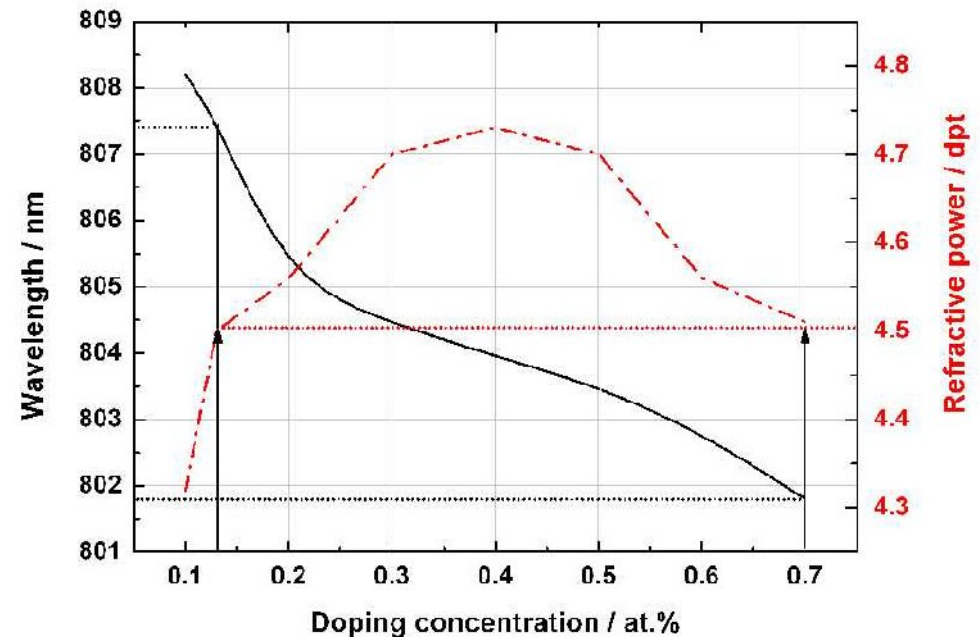
# Highly doped crystals

- Pump wavelength needs to be shifted to get less absorption in order to avoid extreme stresses  
→ which pump wavelength is needed, if everything is supposed to be identical (except the doping) ?



# Highly doped crystals

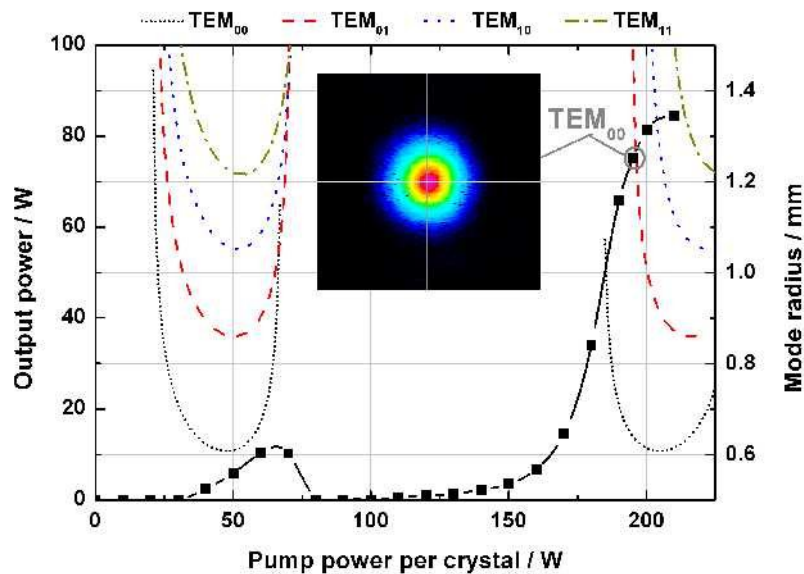
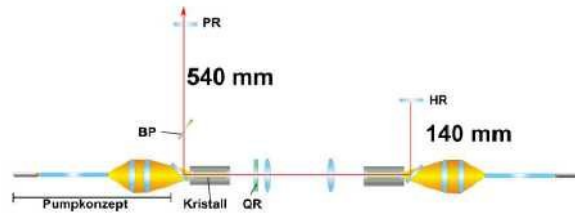
- Pump wavelength needs to be shifted to get less absorption in order to avoid extreme stresses  
→ which pump wavelength is needed, if everything is supposed to be identical (except the doping) ?



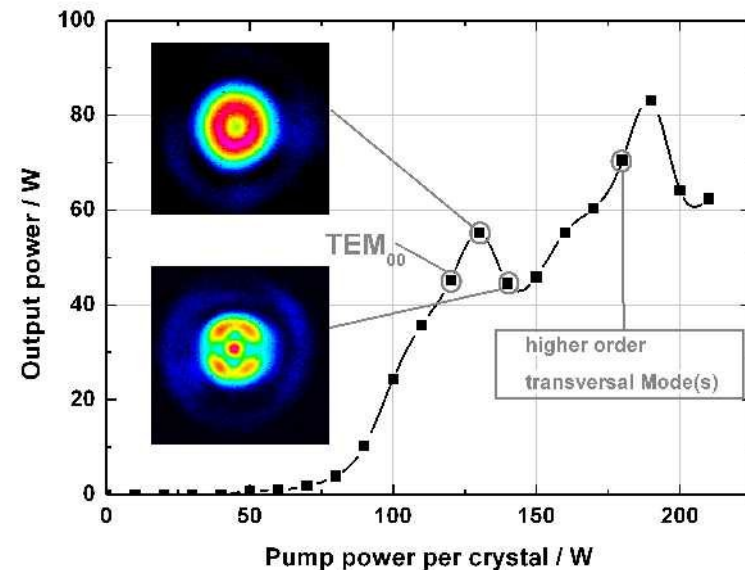
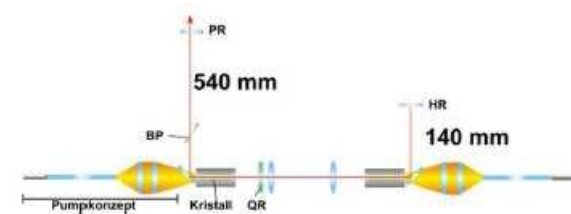
Note: this calculation is based on a constant heat fraction!

# Highly doped crystals

- Comparison with standard crystal – in identical setups



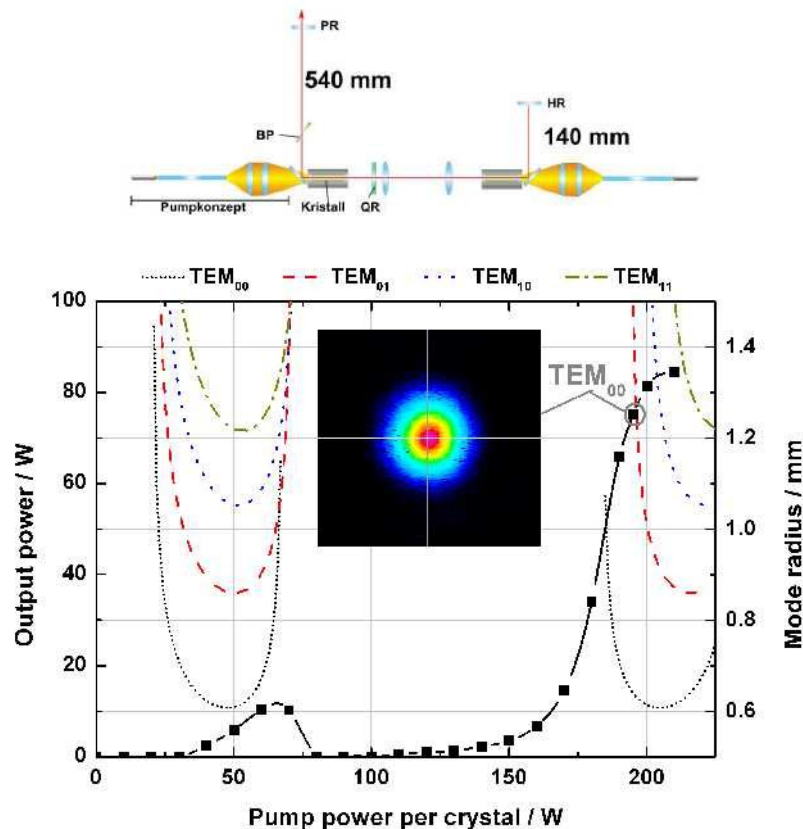
0.13 at.%, 808 nm



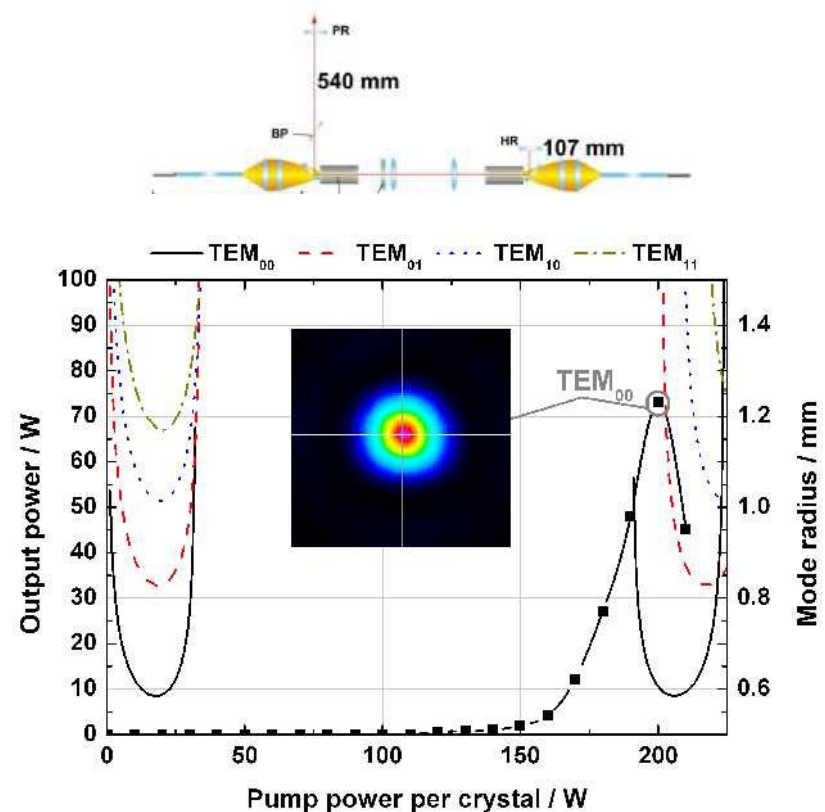
0.68 at.%, 802 nm

# Highly doped crystals

- Comparison with standard crystal – in adapted setups



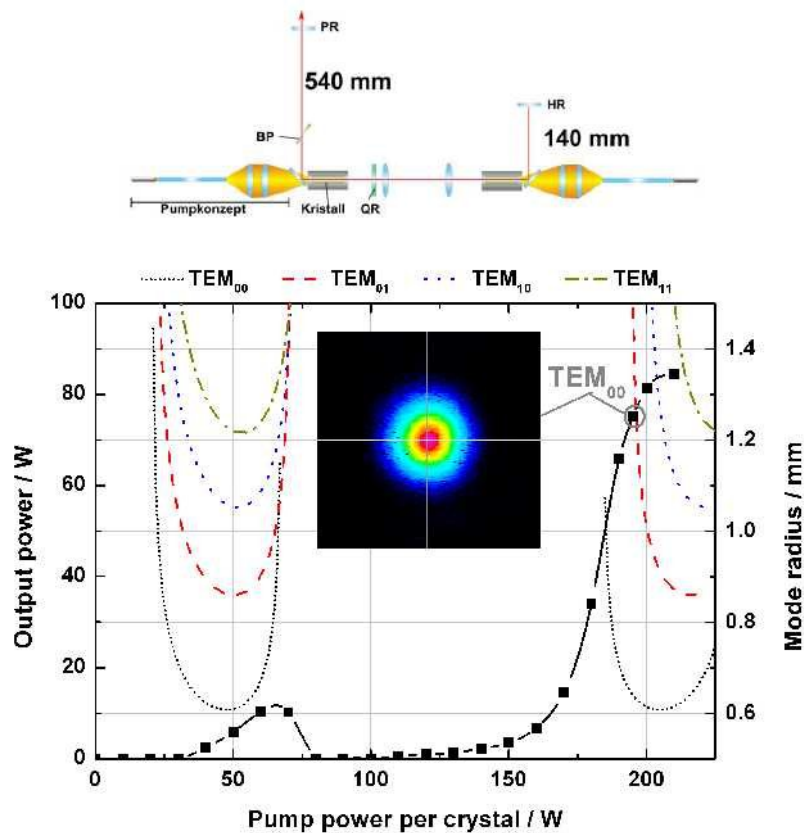
0.13 at.%, 808 nm



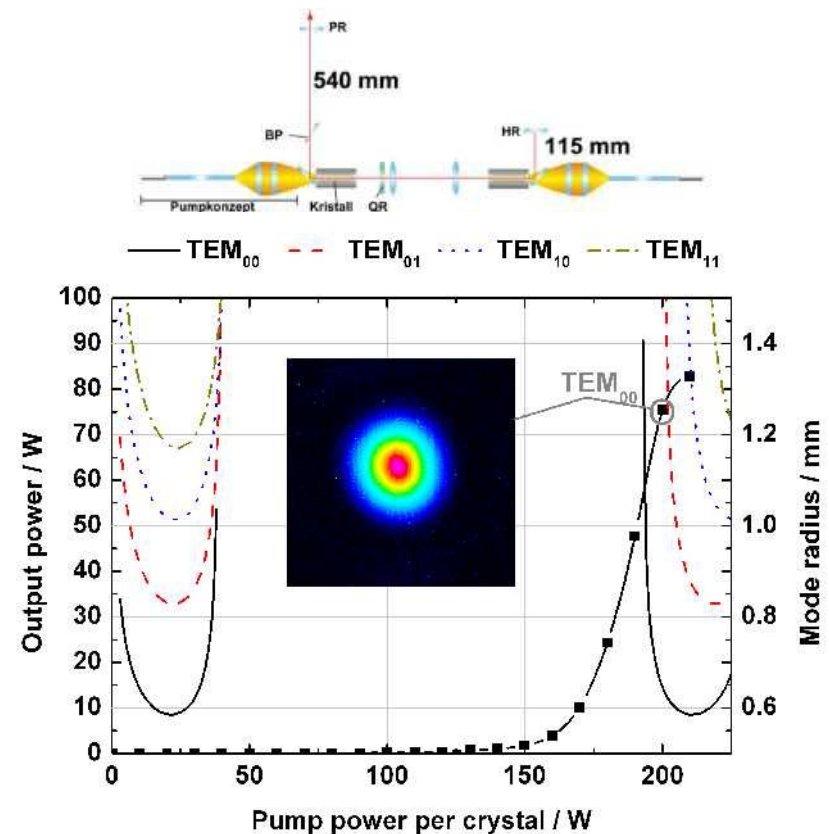
0.68 at.%, 802 nm

# Highly doped crystals

- Comparison with standard crystal – in adapted setups



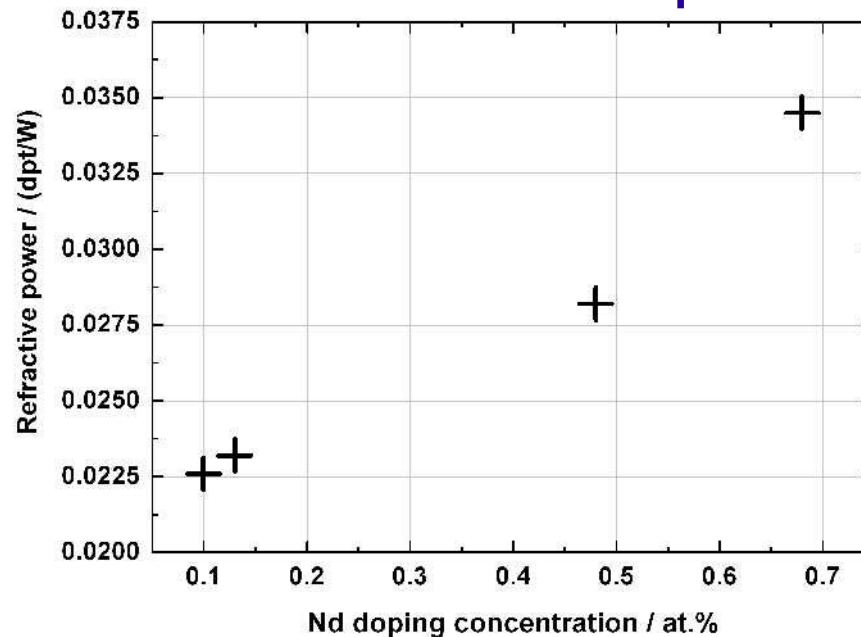
0.13 at.%, 808 nm



0.48 at.%, 802 nm

# Highly doped crystals

- Learned from these Experiments:
  - Thermal refractive power can be estimated from the resonator length
  - The fraction of pump light, converted into heat can be estimated from the refractive power

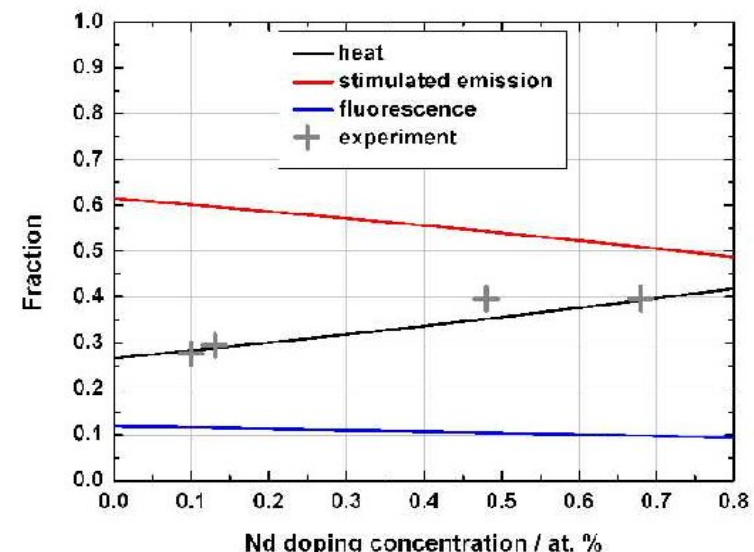




# Highly doped crystals

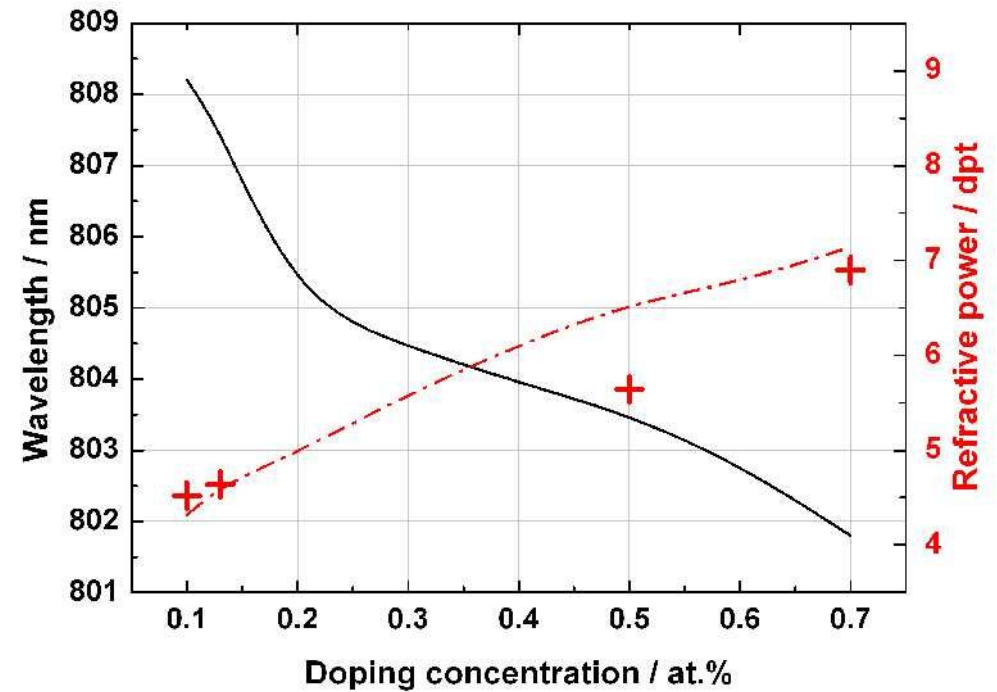
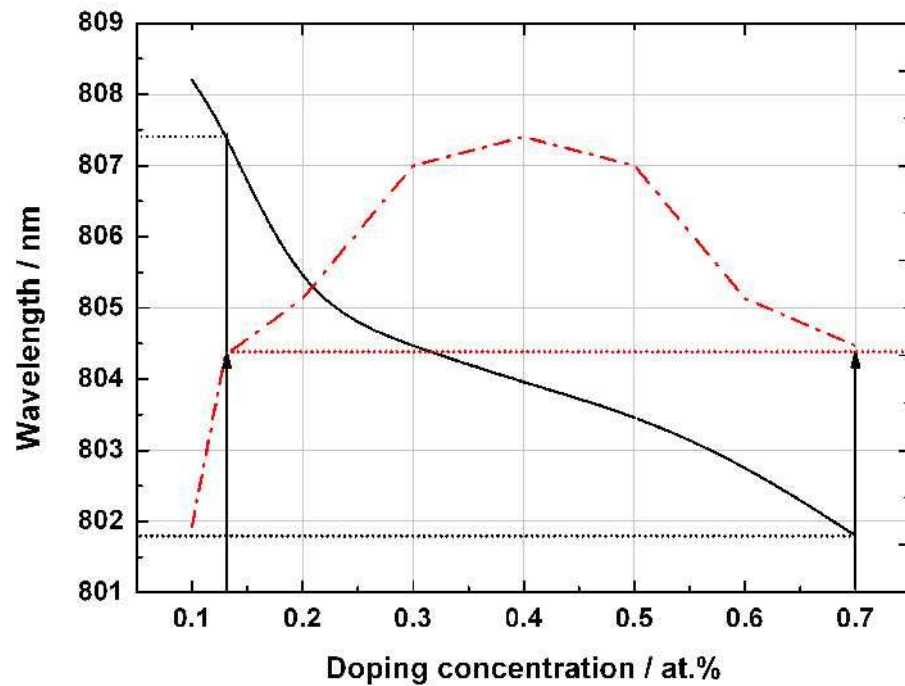
- Learned from these Experiments:
  - Thermal refractive power can be estimated from the resonator length
  - The fraction of pump light, converted into heat can be estimated from the refractive power
  - The fraction of fluorescence, stimulated emission, and inactive Nd ions ("dead sites") can be estimated

Here:  
22% of the ions  
are assumed to be  
optically inactive





# Highly doped crystals: non-constant heat coefficient

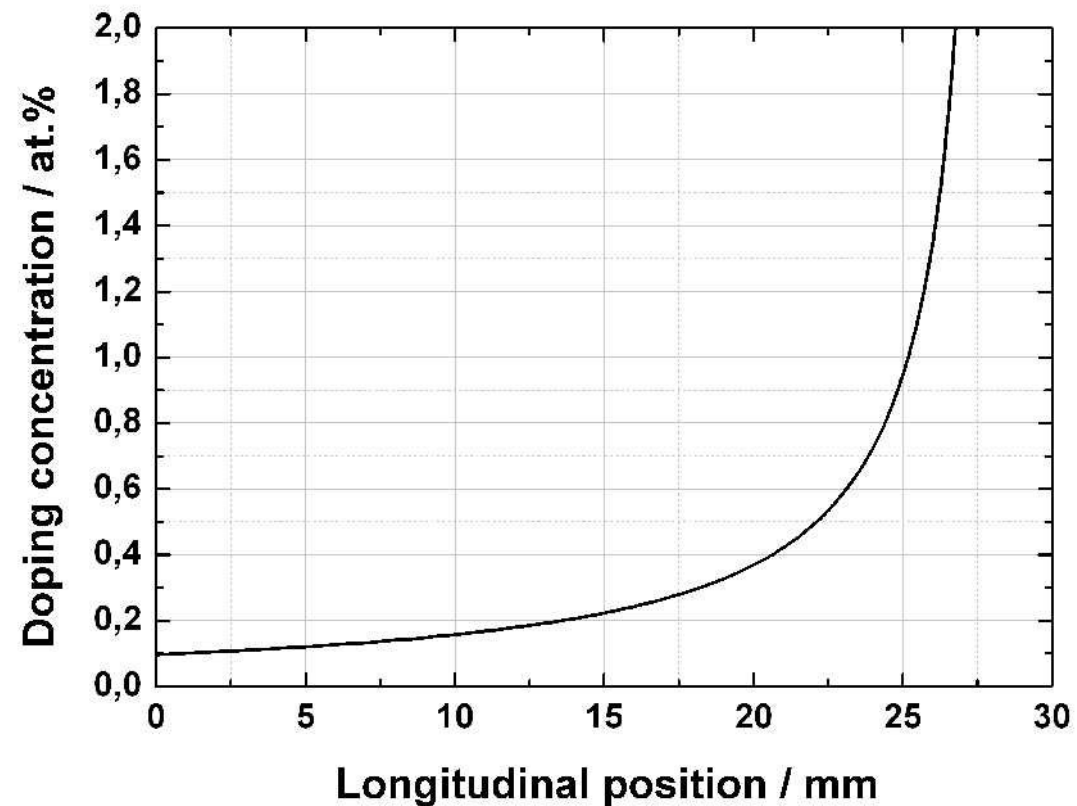


# Outline

- **Overview on thermo-optical effects in lasers**
  - Thermal lensing
  - Birefringence
  - Depolarization
- Aberrations and the PSL working point
- **Attempts for optimization of the laser crystals**
  - Different doping concentrations
  - **Segmented crystals**
  - Intrinsic depolarization compensation

# Segmented crystals

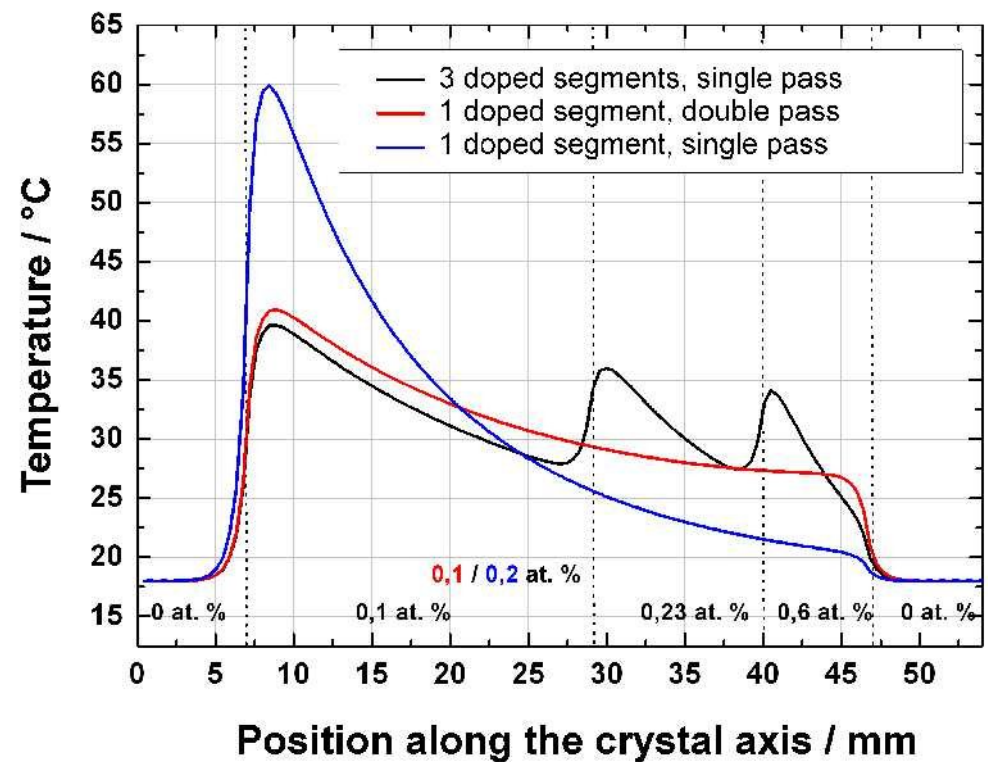
- The maximal pump power (and therefore output power) is limited by the induced heat and occurring stresses
  - Longitudinally homogeneous temperature distribution
  - Optimum: longitudinal hyperbolic doping gradient\* (Figure: 807 nm, FWHM 2.5 nm, 95% absorption)
- ☹ complex manufacturing process



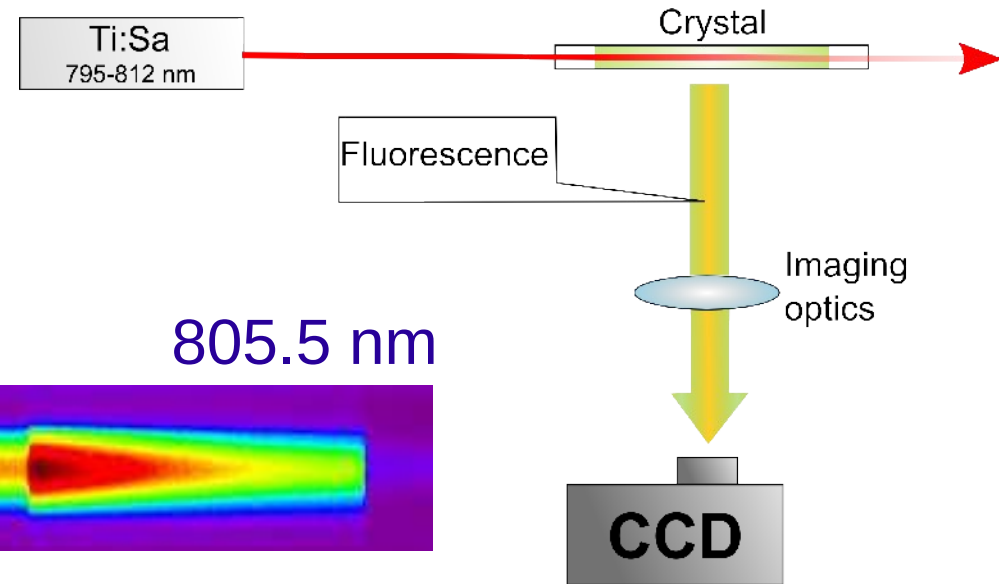
# Segmented crystals

- ☺ Tradeoff: segmented crystals
  - Pump wavelength: 807.8 nm
  - Doped length: 40 mm
  - 3 doped segments

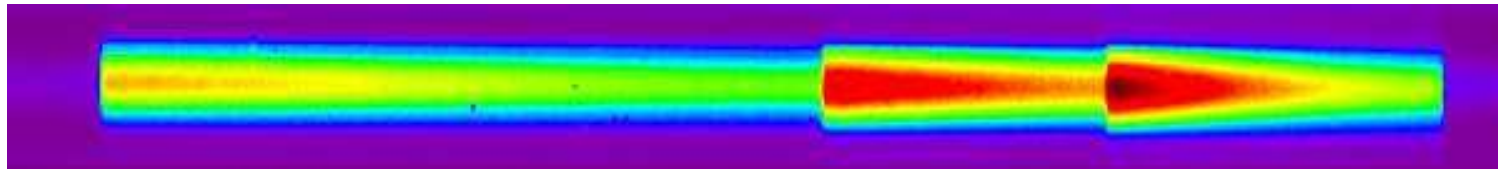
Segment	Length	Doping
1	7 mm	0 at. %
2	22 mm	0.1 at. %
3	11 mm	0.23 at. %
4	7 mm	0.6 at. %
5	7 mm	0 at. %



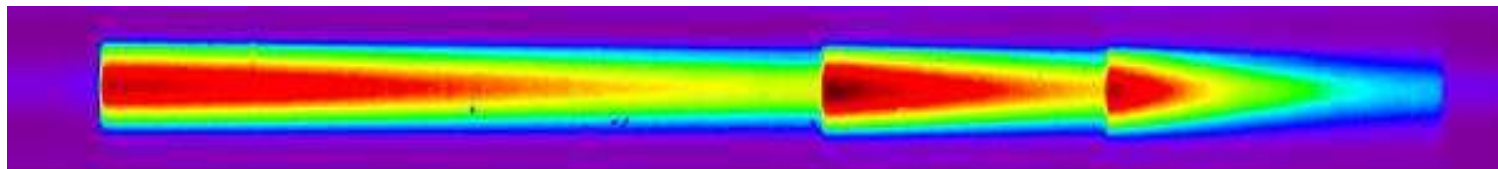
# Optimal pump wavelength



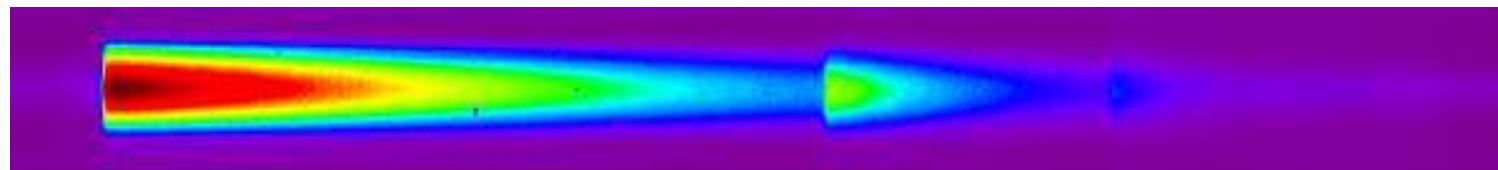
805.5 nm



807 nm

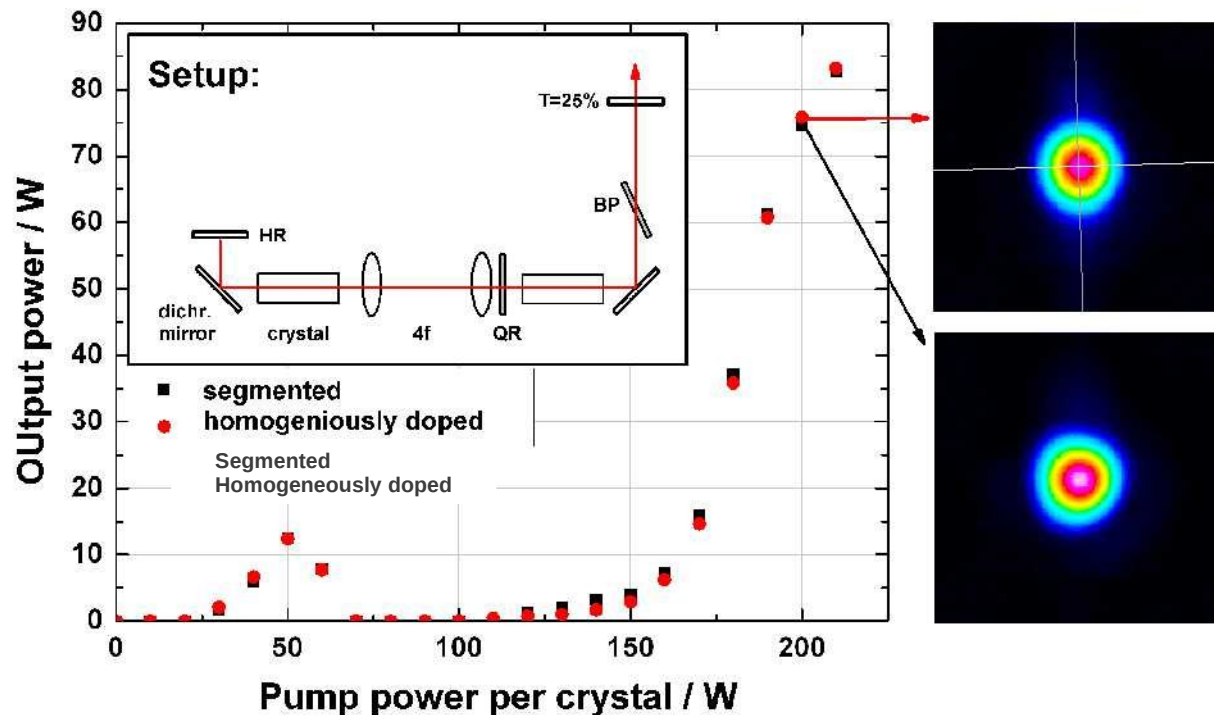


808.5 nm



# Segmented crystals

- Comparison with "standard crystal"

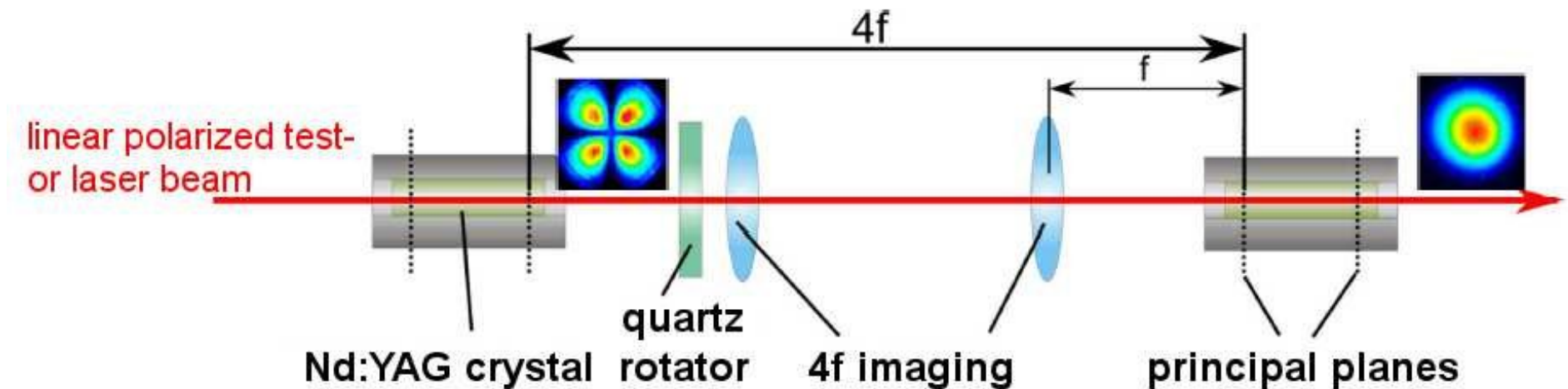


- No difference in laser performance
- No pump light double-pass
- Complex in manufacturing

# Outline

- **Overview on thermo-optical effects in lasers**
  - Thermal lensing
  - Birefringence
  - Depolarization
- Aberrations and the PSL working point
- **Attempts for optimization of the laser crystals**
  - Different doping concentrations
  - Segmented crystals
  - **Intrinsic depolarization compensation**

# Standard birefringence compensation



- + very effective  
(depolarization losses  $< 1\%$ )
- - Additional components inside the resonator  
(absorption, thermal effects, spots,...)
- - Alignment sensitivity



# Intrinsic birefringence reduction

**Pumped crystal becomes birefringent**

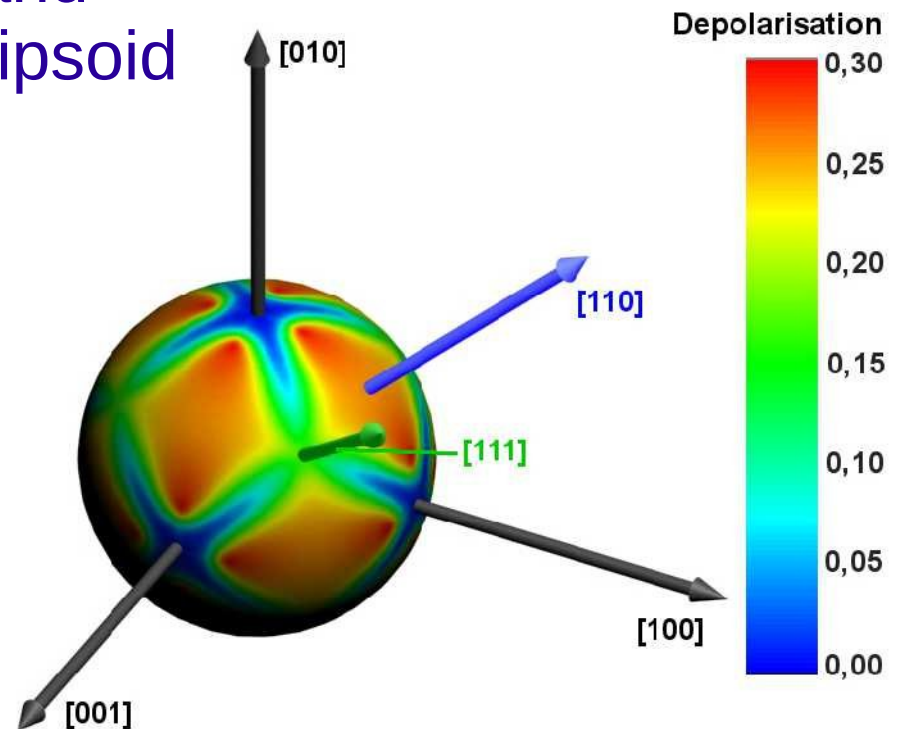
→ **Depolarisation  $D$**

$$D(x,y) = \sin^2(2(\theta(x,y) - \gamma)) \sin^2(\psi(x,y)/2)$$

**$\theta$**  Angle between input polarization and principal axis of the birefringence ellipsoid

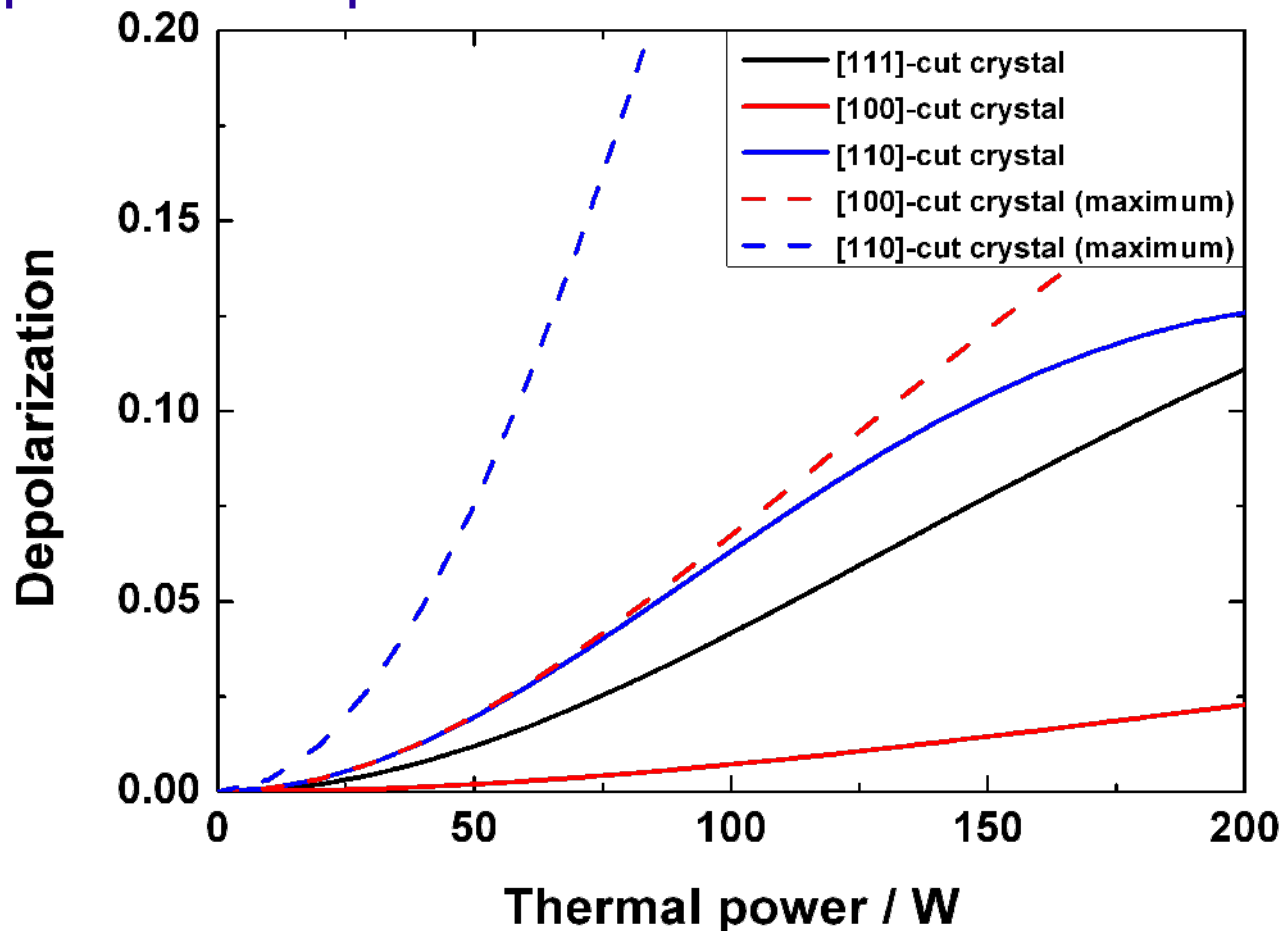
**$\gamma$**  Angle between input polarization and x-axis of the reference system

**$\psi$**  Phase-shift between radial and tangential polarization, **depends on crystal cut!**



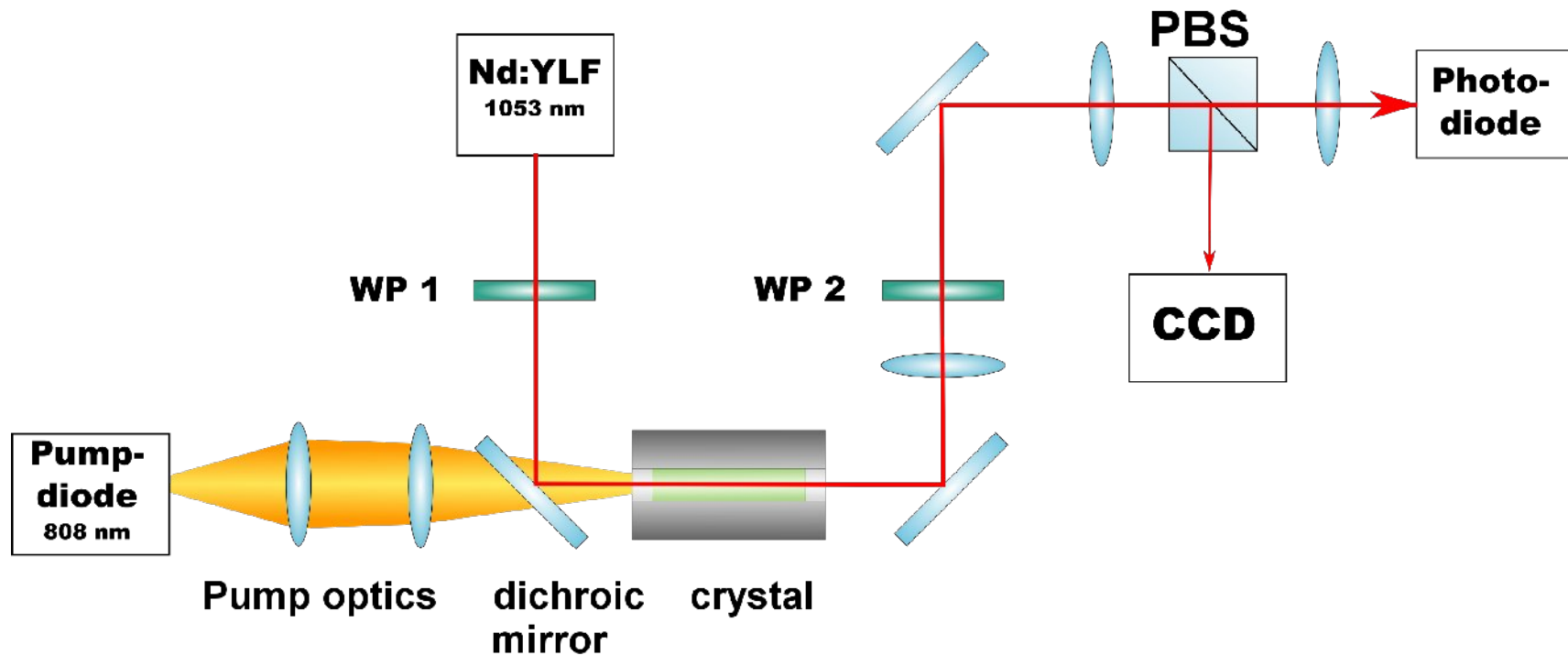
# Intrinsic birefringence reduction

- For [100]- and [110]-cut crystals:  
The depolarization depends on the orientation of the crystal with respect to the polarization orientation of the laser



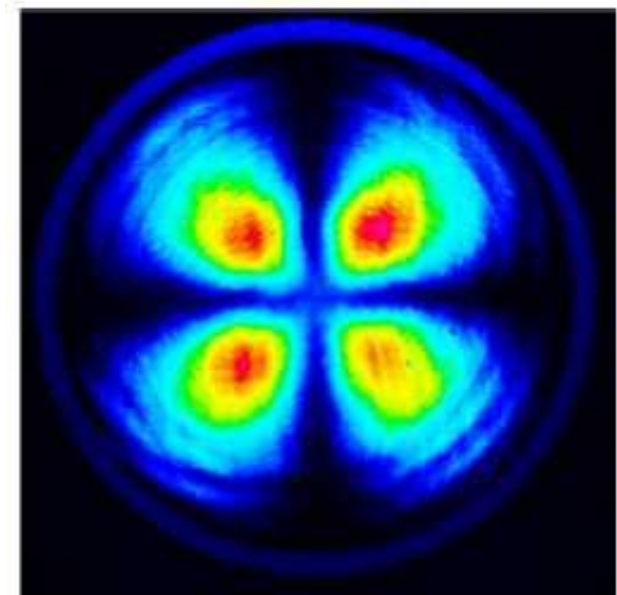
# Investigations with test laser

- Wavelength: 1053 nm
  - No amplification in pumped Nd:YAG crystal
  - Close to Nd:YAG laser wavelength



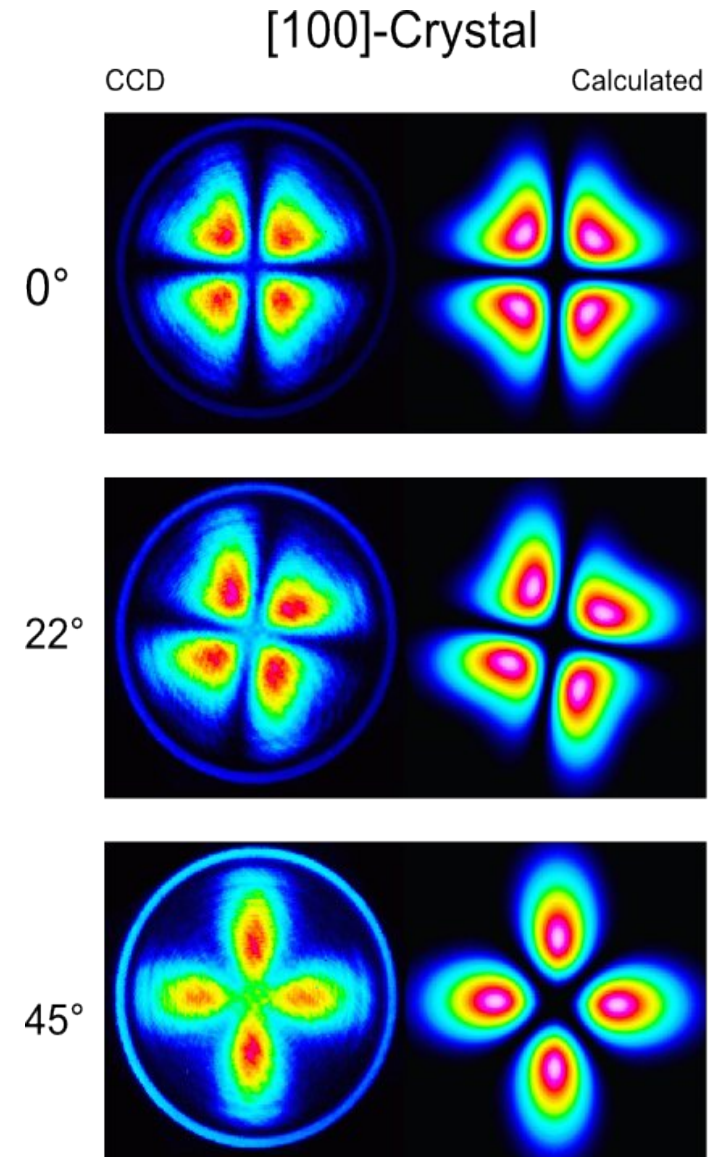
# Investigations with test laser

- [111]-cut: beam pattern rotates



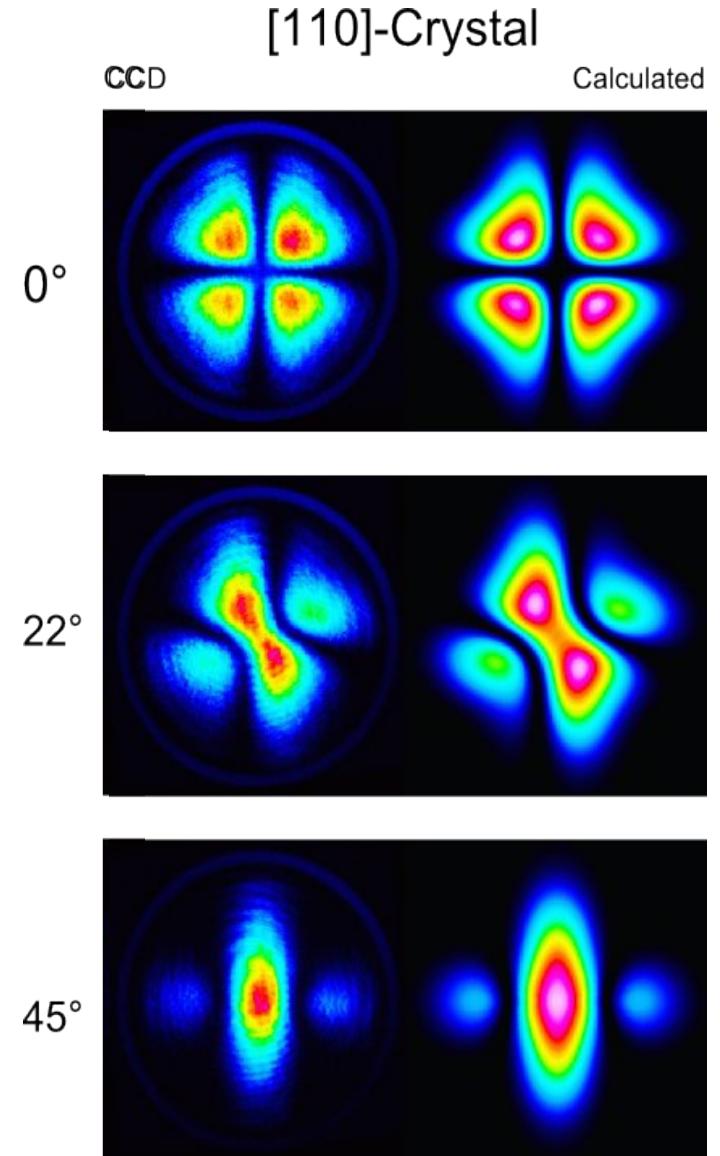
# Investigations with test laser

- [111]-cut: beam pattern rotates
- [100]-cut: beam pattern changes with respect to input polarization  
Principal axis of the refractive index ellipsoid are no longer radially/tangentially oriented

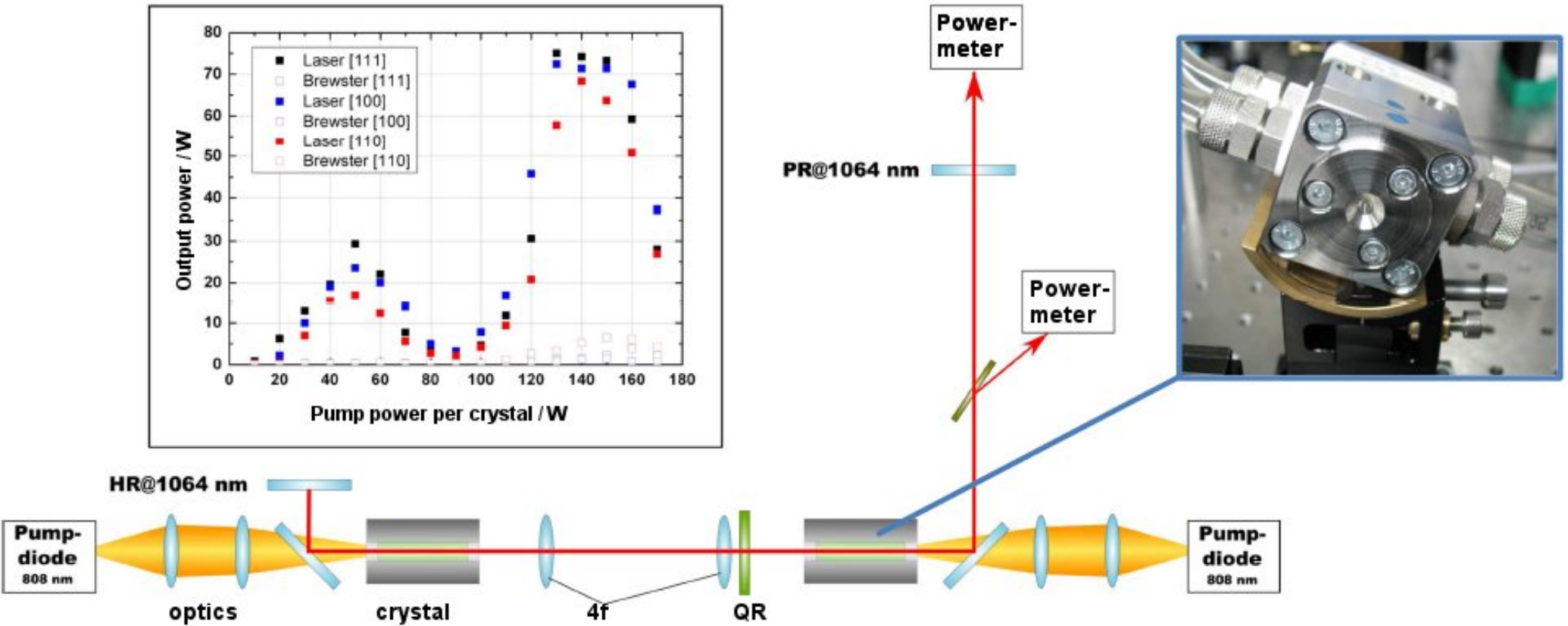
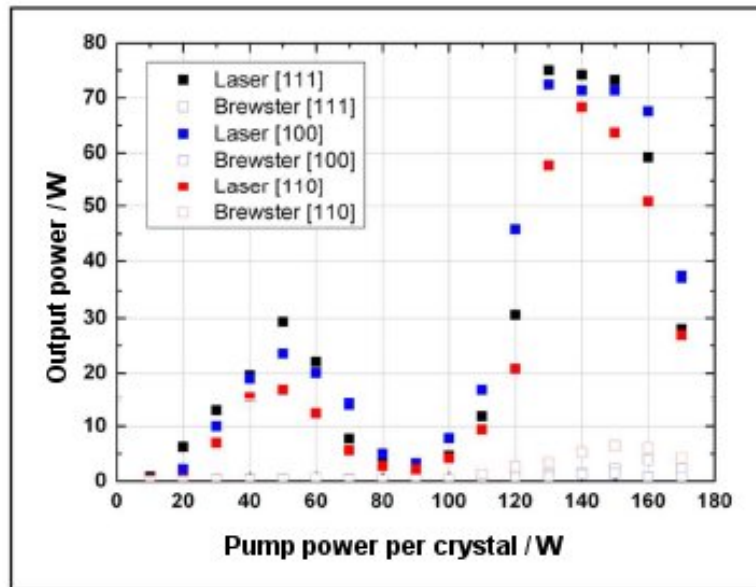


# Investigations with test laser

- [111]-cut: beam pattern rotates
- [100]-cut: beam pattern changes with respect to input polarization  
Principal axis of the refractive index ellipsoid are no longer radially/tangentially oriented
- [110]-cut: Elliptical pattern at  $45^\circ$  with maximum at the center



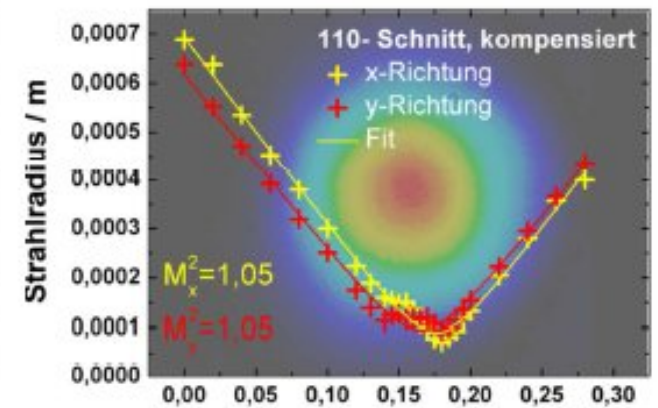
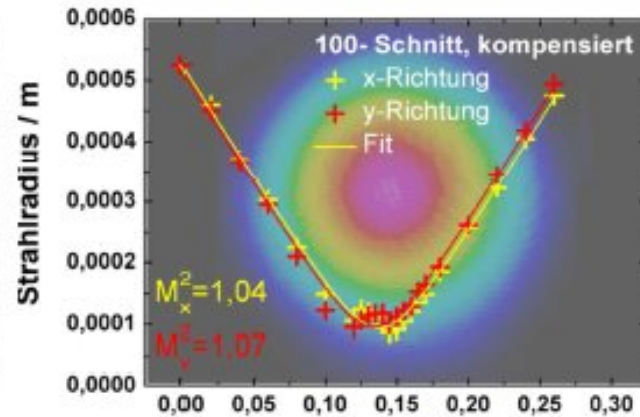
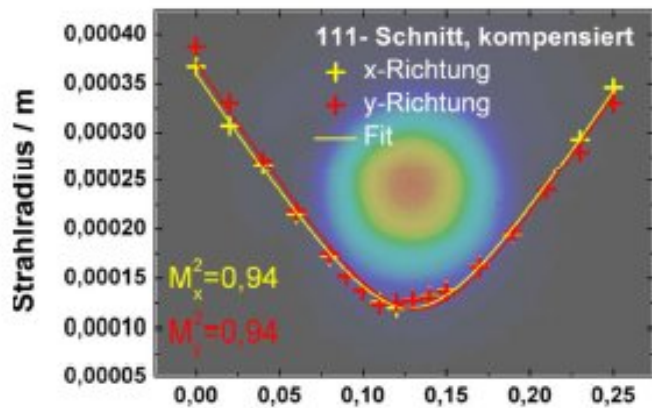
# Investigations with asymmetric two-head laser





# Investigations with asymmetric two-head laser

compensated

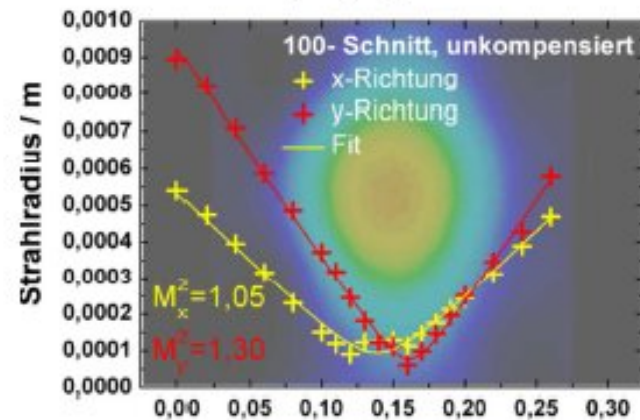
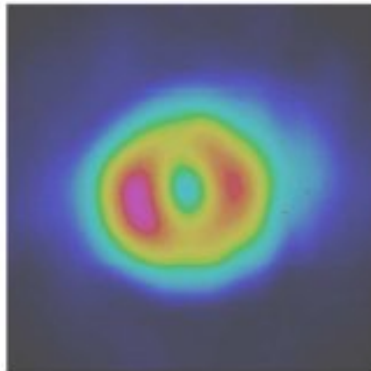


Position in propagation direction / m

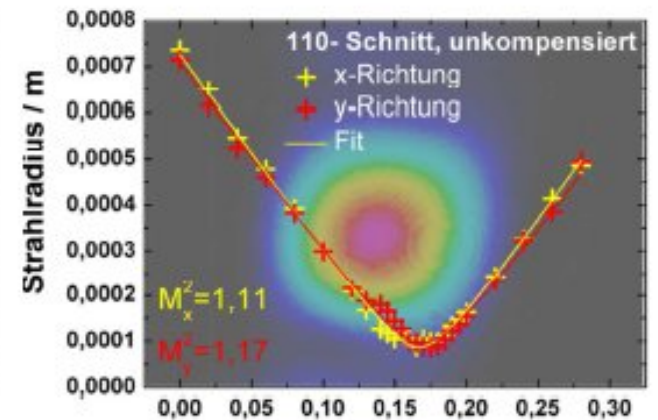
Position in propagation direction / m

Position in propagation direction / m

uncompensated



Position in propagation direction / m



Position in propagation direction / m

**huge depolarization losses!**



# Acknowledgment

## Data and pictures taken from:

(former) LZH researchers: Oliver Puncken, Marcin Damjanic, Maik Frede, Raphael Kluzik, Dietmar Kracht, Bastian Schulz, Christian Veltkamp, Peter Weißels, Ralf Wilhelm, Lutz Winkelmann et al.

(former) AEI researchers: Christina Bogan, Patrick Kwee, Jan Pöld, Frank Seifert, Benno Willke et al.

LIGO Document Control Center (DCC)

## Thanks!